# *Impact of AGN Feedback on Metal Enrichment of the IGM*

**Paramita Barai**


**CosmoComp Workshop - Trieste**

16th March, 2012

# Outline

- Introduction: AGN feedback
  - Trends from observations
  - Modeling in cosmological simulations

- Our work:
  AGN outflows & IGM enrichment
  - Methodology
  - Simulation
  - Results : IGM Volume Enriched & Metallicity

# What is AGN?

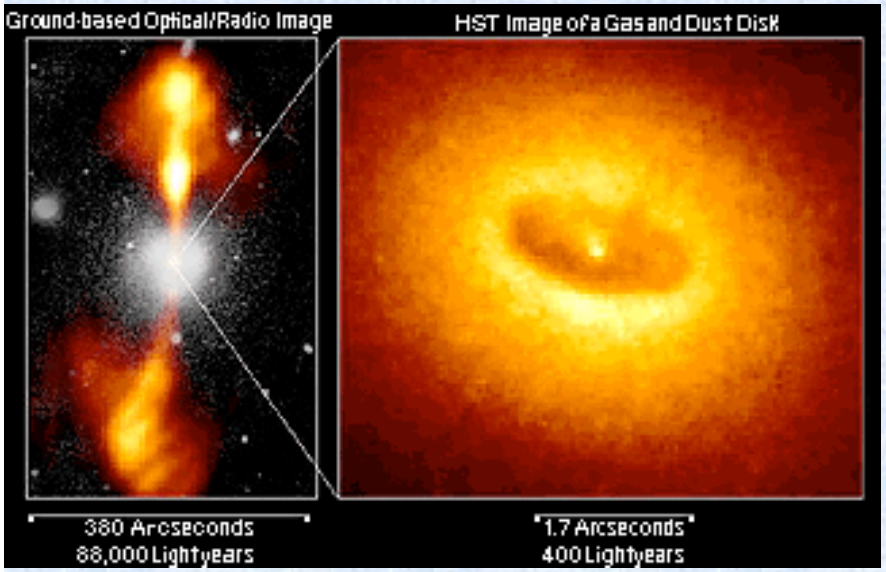


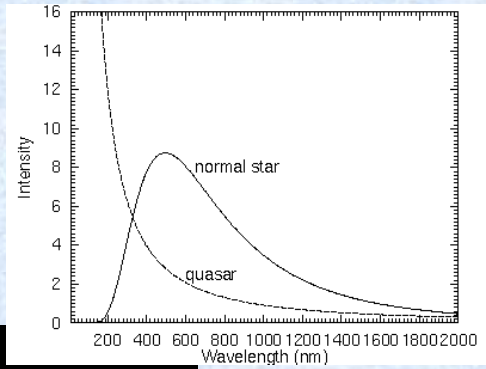


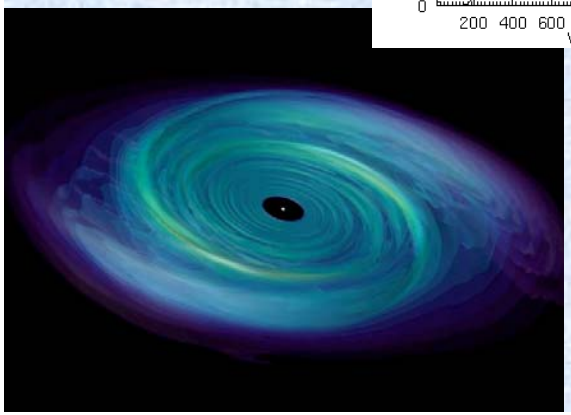

- Active nucleus ⇒ Central region radiates more energy than all the stars in the whole galaxy
- Very high luminosity
  - $10^{44}$ - $10^{46}$ erg $s^{-1}$
- AGN has non-thermal spectrum
  - Not normal evolution of stars
- Powered by gas accretion onto a supermassive black hole (SMBH)
  - $M_{BH} > 10^6 M_{sun}$
  - Release of gravitational energy: Efficient conversion of mass into energy

# The case for AGN Feedback from Observations …

# BH-Galaxy Correlation

- Tight relation between BH mass and host galaxy bulge mass / velocity dispersion

⇒ Formation of BHs and galaxy bulges must be related

(Magorrian, J. et al. 1998, AJ, 115, 2285; Gebhardt, K. et al. 2000, ApJ, 539, L13G; Ferrarese, L. & Merritt, D. 2000, ApJ, 539, L9)

17/03/12

## $M_{BH}$ - σ relation

(Tremaine, S. et al. 2002, ApJ, 574, 740)

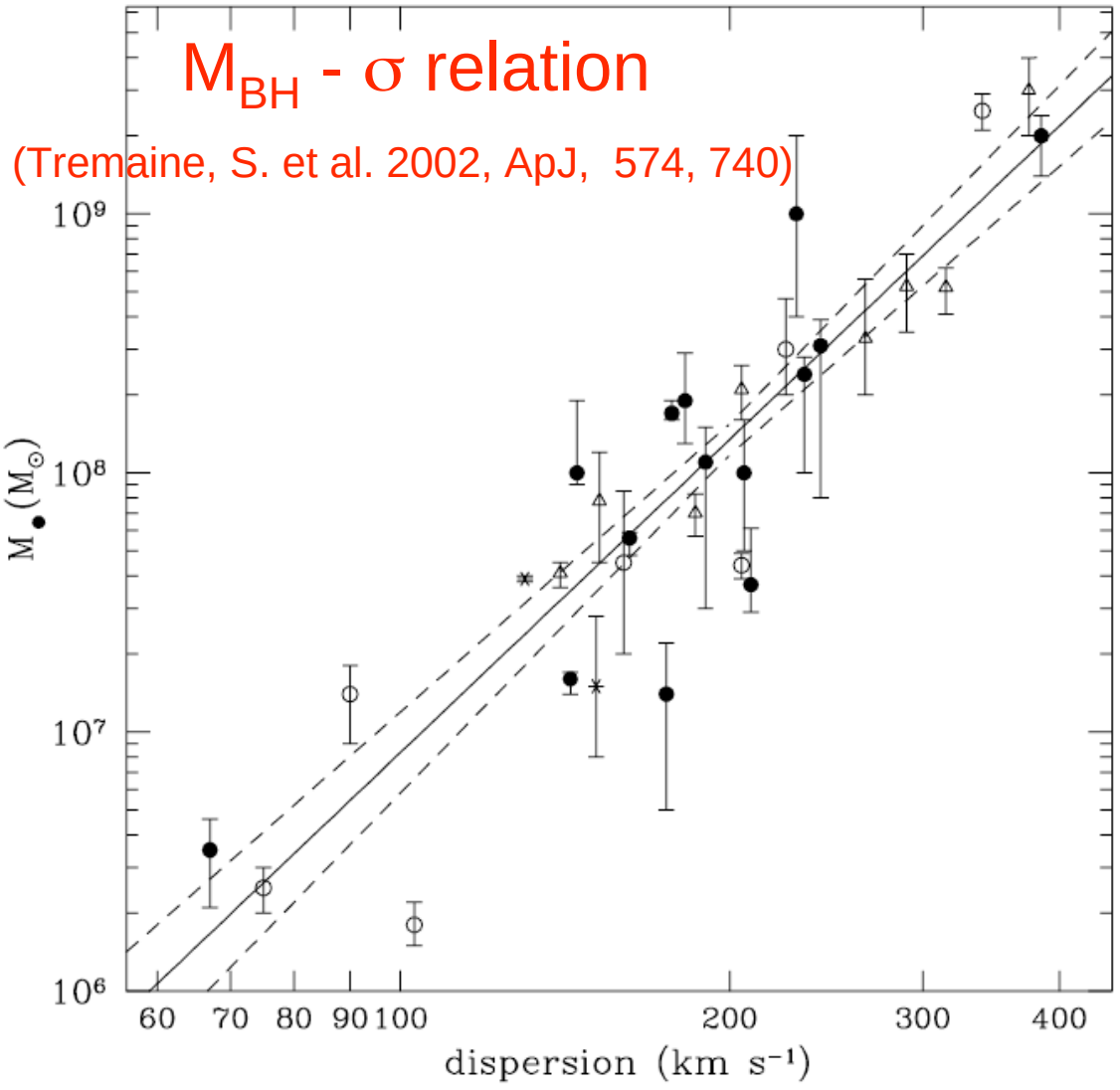


FIG. 7.—Data on black hole masses and dispersions for the galaxies in Table 1, along with the best-fit correlation described by eqs. (1) and (19). Mass measurements based on stellar kinematics are denoted by circles, on gas kinematics by triangles, and on maser kinematics by asterisks; Nuker measurements are denoted by filled circles. The dashed lines show the 1 $\sigma$ limits on the best-fit correlation.

# Redshift Evolution

E RELATION BETWEEN BLACK HOLE MASS AND HOST SPHEROID STELLAR MASS OUT TO $Z \sim 2$

VARDHA N. BENNERT[1,2], MATTHEW W. AUGER[1], TOMMASO TREU[1,3], JONG-HAK WOO[4], MATTHEW A. MALKAN[5]

*Draft version October 18, 2011*

(2011, ApJ, 742, 107)

ABSTRACT

We combine Hubble Space Telescope images from the Great Observatories Origins Deep Survey with archival Very Large Telescope and Keck spectra of a sample of 11 X-ray selected broad-line active galactic nuclei in the redshift range $1 < z < 2$ to study the black hole mass - stellar mass relation out to a lookback time of 10 Gyrs. Stellar masses of the spheroidal component ($M_{\rm sph,\star}$) are derived from multi-filter surface photometry. Black hole masses ($M_{\rm BH}$) are estimated from the width of the broad MgII emission line and the 3000Å nuclear luminosity. Comparing with a uniformly measured local sample and taking into account selection effects, we find evolution in the form $M_{\rm BH}/M_{\rm sph,\star} \propto (1+z)^{1.96\pm0.55}$, in agreement with our earlier studies based on spheroid luminosity. However, this result is more accurate because it does not require a correction for luminosity evolution and therefore avoids the related and dominant systematic uncertainty. We also measure total stellar masses ($M_{\rm host,\star}$). Combining our sample with data from the literature, we find $M_{\rm BH}/M_{\rm host,\star} \propto (1+z)^{1.15\pm0.15}$, consistent with the hypothesis that black holes (in the range $M_{\rm BH} \sim 10^{8-9} M_\odot$) predate the formation of their host galaxies. Roughly one third of our objects reside in spiral galaxies; none of the host galaxies reveal signs of interaction or major merger activity. Combined with the slower evolution in host stellar masses compared to spheroid stellar masses, our results indicate that secular evolution or minor mergers play a non-negligible role in growing both BHs and spheroids.

# Co-Evolution (of Galaxies & AGN)

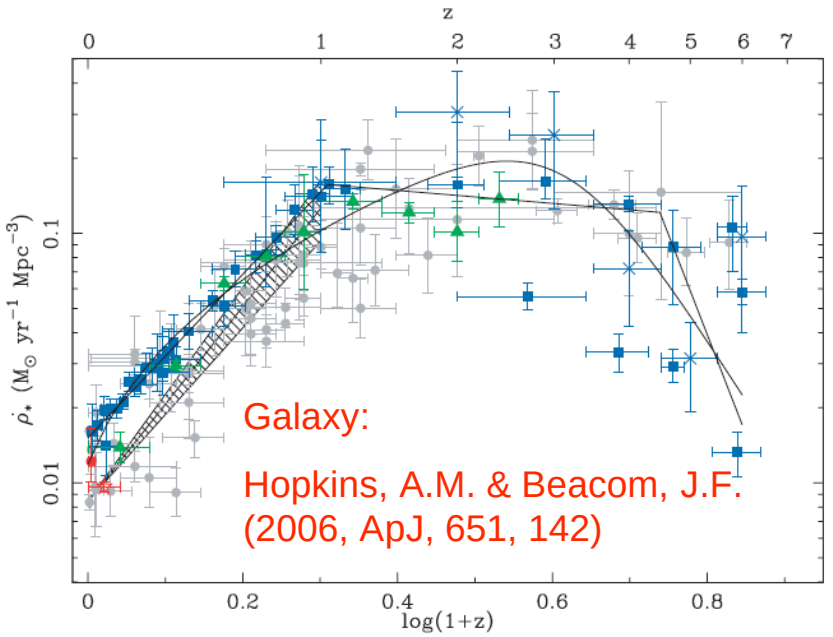


FIG. 1.— Evolution of SFR density with redshift. Data shown here have been scaled, assuming the SalA IMF. The gray points are from the compilation of Hopkins (2004). The hatched region is the FIR (24 $\mu$m) SFH from Le Floc'h et al. (2005). The green triangles are FIR (24 $\mu$m) data from Pérez-González et al. (2005). The open red star at $z = 0.05$ is based on radio (1.4 GHz) data from Mauch (2005). The filled red circle at $z = 0.01$ is the H$\alpha$ estimate from Hanish et al. (2006). The blue squares are UV data from Baldry et al. (2005), Wolf et al. (2003), Arnouts et al. (2005), Bouwens et al. (2003a, 2003b, 2005a), Bunker et al. (2004), and Ouchi et al. (2004). The blue crosses are the UDF estimates from Thompson et al. (2006). Note that these have been scaled to the SalA IMF, assuming they were originally estimated using a uniform Salpeter (1955) IMF. The solid lines are the best-fitting parametric forms (see text for details of which data are used in the fitting). Although the FIR SFH of Le Floc'h et al. (2005) is not used directly in the fitting, it has been used to effectively obscuration-correct the UV data to the values shown, which are used in the fitting. Note that the top logarithmic scale is labeled with redshift values, not $(1 + z)$.

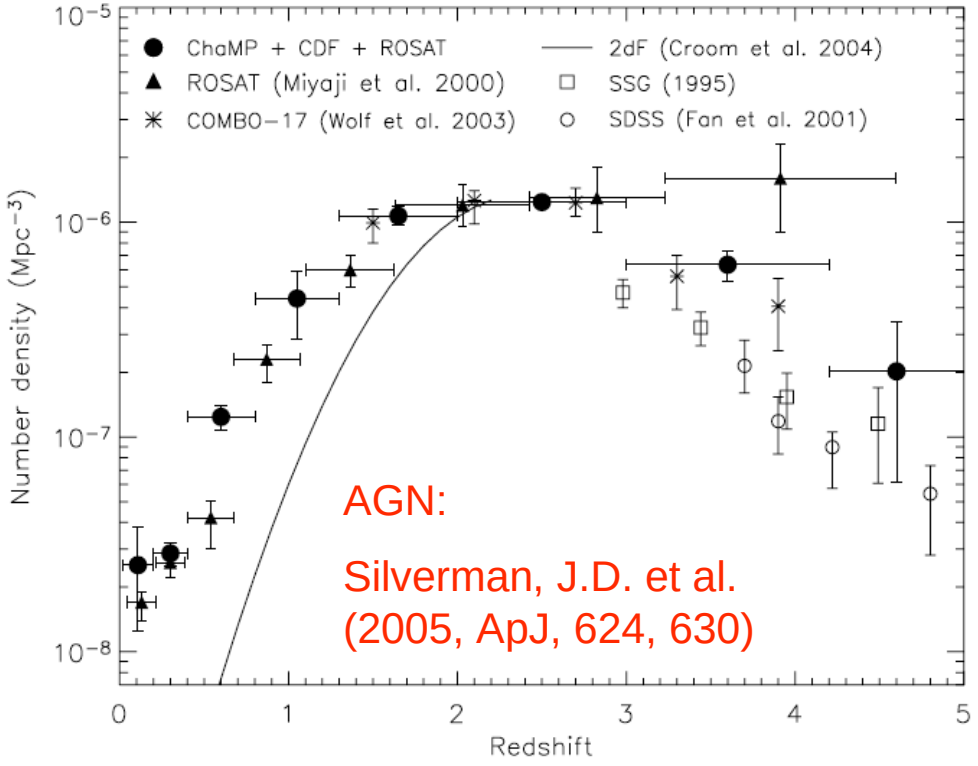


FIG. 9.— Comoving space density of 217 *Chandra* + *ROSAT* AGNs selected in the soft (0.5–2.0 keV) band with $\log L_X > 44.5$ compared to the optical surveys. The optical space densities have been scaled to match the X-ray points at $z = 2.5$ for ease of comparison.

- Can we link up the cosmological evolution of galaxy & AGN populations?

# Star-Formation Quenched by AGN activity

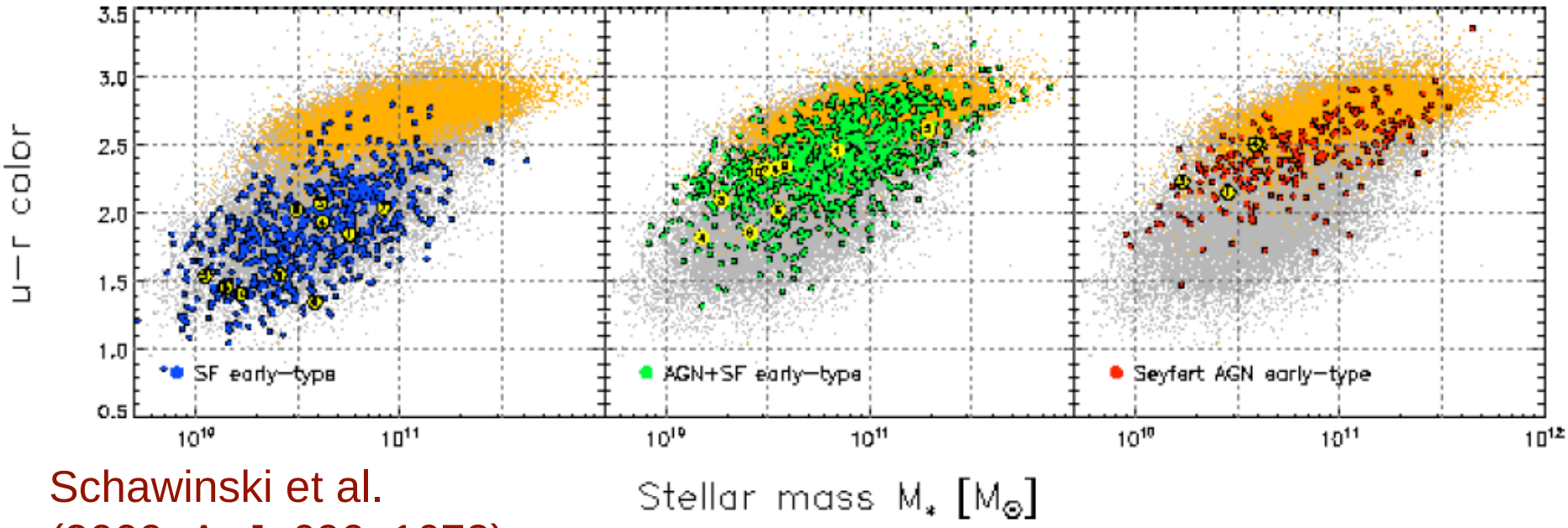


Schawinski et al.
(2009, ApJ, 690, 1672)

FIG. 1.— The color-mass relationship for the galaxies in our sample. We plot the galaxy stellar mass derived by spectral energy distribution fitting using the models of Maraston (2005), versus the optical $u - r$ color. In each panel, morphological late-types are gray, quiescent early-types are orange and the various active early-types (classified by optical emission line ratios) are colored in in each panel. From left to right: blue (SF), green (AGN+SF), red (Seyfert AGN). We mark the galaxies observed with the IRAM 30m telescope with larger points, number them and show their SDSS *gri* composite color images (Lupton et al. 2004) below in three blocks corresponding to the three classifications. This Figure illustrates the progression of early-type galaxies from the blue cloud of starforming galaxies via an AGN phase to the red sequence of passive galaxies.

# *How do AGN affect their Host Galaxies & the large-scale* IGM*?*

- In the form of Feedback
- Mass accreted in at rate $dM_{BH}/dt$

- Energy-driven: fraction of radiated energy is coupled to the surroundings
  - Heating / thermal coupling
  - Kinetic / mechanical outflow
  - …

$$\dot{E}_{feedback} = \varepsilon_f L_{radiated} = \varepsilon_f \varepsilon_r \dot{M}_{BH} c^2$$

$\varepsilon_r = 0.1$ ... Schwarzschild BH

$\varepsilon_r = 0.4$ ... Kerr BH

- Momentum-driven $\dot{M}_{out} \propto \dot{M}_{BH}$

(Shakura & Sunyaev 1973, A&A, 24, 337)

- Exact details are unknown

A&A 491, 407–424 (2008)
DOI: 10.1051/0004-6361:200810346
© ESO 2008

Astronomy & Astrophysic

# Evidence for powerful AGN winds at high redshift: dynamics of galactic outflows in radio galaxies during the "Quasar Era"⋆

N. P. H. Nesvadba[1,2], M. D. Lehnert[1], C. De Breuck[3], A. M. Gilbert[4], and W. van Breugel[5]

[1] GEPI, Observatoire de Paris, CNRS, Université Denis Diderot, 5 place Jules Janssen, 92190 Meudon, France
e-mail: nicole.nesvadba@obspm.fr
[2] Marie-Curie Fellow
[3] European Southern Observatory, Karl-Schwarzschild Strasse, 85748 Garching bei München, Germany
[4] The Aerospace Corporation, PO Box 92957, MS M2-266, El Segundo, CA 90245, USA
[5] University of California, Merced, PO Box 2039, Merced, CA 95344, USA

Recieved 8 June 2008 / Accepted 30 August 2008

**ABSTRACT**

AGN feedback now appears as an attractive mechanism to resolve some of the outstanding problems with the "standard" cosmological models, in particular those related to massive galaxies. At low redshift, evidence is growing that gas cooling and star formation may be efficiently suppressed by mechanical energy input from radio sources. To directly constrain how this may influence the formation of massive galaxies near the peak in the redshift distribution of powerful quasars, $z \sim 2$, we present an analysis of the emission-line kinematics of 3 powerful radio galaxies at $z \sim 2$–3 (HzRGs) based on rest-frame optical integral-field spectroscopy obtained with SINFONI on the VLT. The host galaxies of powerful radio-loud AGN are among the most massive galaxies, and thus AGN feedback may have a particularly clear signature in these galaxies.

We find evidence for bipolar outflows in all HzRGs, with kinetic energies equivalent to 0.2% of the rest-mass of the supermassive black hole. Observed total velocity offsets in the outflows are ~800–1000 km s$^{-1}$ between the blueshifted and redshifted line emission, and *FWHM*s ~ 1000 km s$^{-1}$ suggest strong turbulence. Line ratios indicate electron temperatures, ~$10^4$ K from [OIII]$\lambda\lambda\lambda$4363, 4959, 5007 at $z \sim 2$, electron densities (~500 cm$^{-3}$) and extinction ($A_V \sim 1$–4 mag). Ionized gas masses estimated from the H$\alpha$ luminosity are of order $10^{10}$ $M_\odot$, similar to the molecular gas content of HzRGs, underlining that these outflows may indicate a significant phase in the evolution of the host galaxy. The total energy release of ~$10^{60}$ erg during a dynamical time of ~$10^7$ yrs corresponds to about the binding energy of a massive galaxy, similar to the prescriptions adopted in galaxy evolution models. Geometry, timescales and energy injection rates of order 10% of the kinetic energy flux of the jet suggest that the outflows are most likely driven by the radio source. The global energy density release of ~$10^{57}$ erg s$^{-1}$ Mpc$^{-3}$ may also influence the subsequent evolution of the HzRG by enhancing the entropy and pressure in the surrounding halo and facilitating ram-pressure stripping of gas in satellite galaxies that may contribute to the subsequent mass assembly of the HzRG through low-dissipation "dry" mergers.

# *The Feedback Loop in a Galaxy*

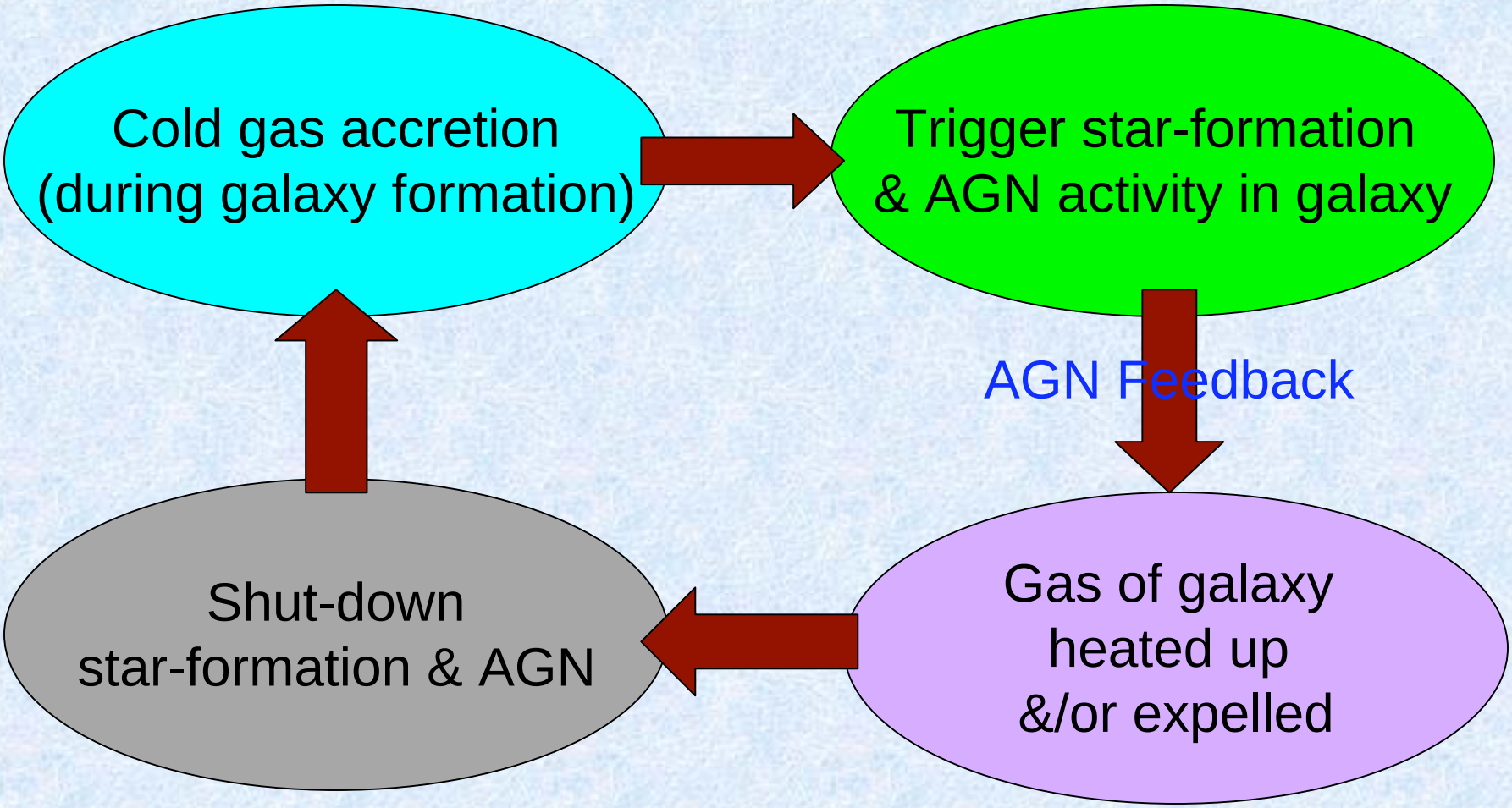

# AGN Feedback in Galaxy Formation / Cosmological Simulations …

# Small-scale Accretion

- BH inner boundary condition: Supersonic flow at Event Horizon (EH)
- Far away from EH – subsonic
- Hence BH accretion is transonic: crosses *Mach* = 1
  - Except cases where already supersonic initially
- Shock Formation → Multi-transonic flow

$$Mach(r) = \frac{v(r)}{c_s(r)}$$

Barai, Das & Wiita (2004, ApJ, 613, L49)

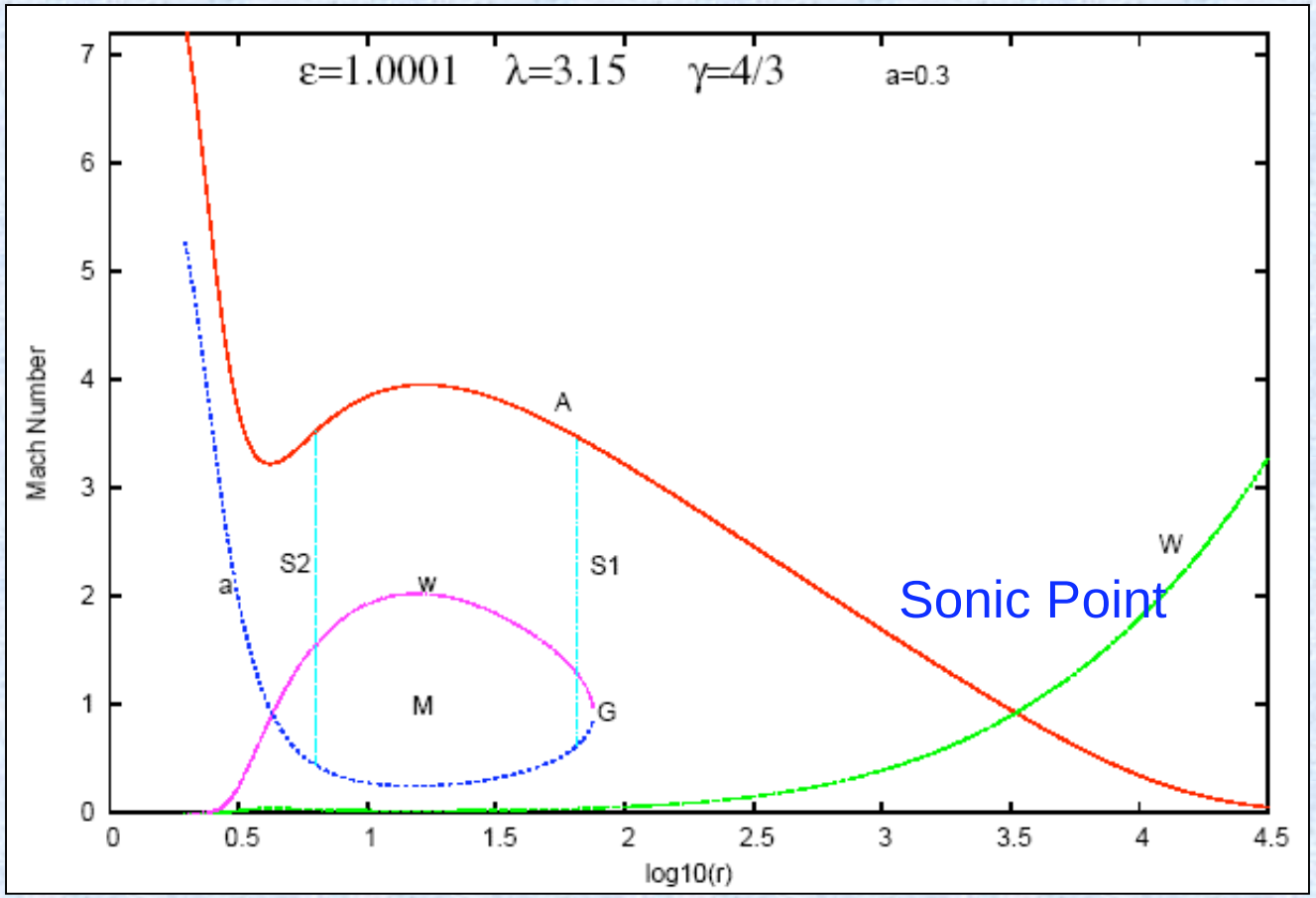

# Subgrid Modeling

- Large dynamic range of length scales
  - BH accretion --- sub-pc
  - Galaxy physics --- kpc
- Computationally challenging
- Cosmological simulations cannot resolve the Sonic Point, which is important to properly model BH accretion

- Physical Processes
  - Accretion of gas onto SMBH
  - Feedback
    - Thermal
    - Kinetic
- Existing subgrid models of AGN feedback assume ad-hoc choice of parameter values

Mon. Not. R. Astron. Soc. **361,** 776–794 (2005) doi:10.1111/j.1365-2

# Modelling feedback from



Like our procedure for coarse graining flexible and can be applied to any model starting point, we relate the (unresolved) a the large-scale (resolved) gas distribution Lyttleton parametrization (Hoyle & Lyttlet 1944; Bondi 1952). In this description, the BH is given by

$$\dot{M}_{\rm B} = \frac{4\pi\,\alpha\,G^2 M_{\rm BH}^2\,\rho}{\left(c_{\rm s}^2 + v^2\right)^{3/2}},$$

$\alpha = 1 - 100$

where $\rho$ and $c_{\rm s}$ are the density and sound s tively, $\alpha$ is a dimensionless parameter, and BH relative to the gas. We will also assu limited to the Eddington rate

$$\dot{M}_{\rm Edd} \equiv \frac{4\pi\,G\,M_{\rm BH}\,m_{\rm p}}{\epsilon_{\rm r}\,\sigma_{\rm T}\,c},$$

where $m_{\rm p}$ is the proton mass, $\sigma_{\rm T}$ is the Tho $\epsilon_{\rm r}$ is the radiative efficiency. The latter is

luminosity, $L_{\rm r}$, and accretion rate, $\dot{M}_{\rm BH}$, by

$$\epsilon_{\rm r} = \frac{L_{\rm r}}{\dot{M}_{\rm BH}\,c^2}, \tag{32}$$

i.e. it simply gives the mass to energy conversion efficiency set by the amount of energy that can be extracted from the innermost stable orbit of an accretion disc around a BH. For the rest of this study, we adopt a fixed value of $\epsilon_{\rm r} = 0.1$, which is the mean value radiatively efficient Shakura & Sunyaev (1973) accretion onto a Schwarzschild BH. We ignore the possibility of radiatively inefficient accretion phases. The accretion rate is then

$$\dot{M}_{\rm BH} = \min(\dot{M}_{\rm Edd}\,,\ \dot{M}_{\rm B}). \tag{33}$$

We will assume that some fraction $\epsilon_{\rm f}$ of the radiated luminosity $L_{\rm r}$ can couple thermally (and isotropically) to surrounding gas in the form of feedback energy, viz.

$$\dot{E}_{\rm feed} = \epsilon_{\rm f}\,L_{\rm r} = \epsilon_{\rm f}\,\epsilon_{\rm r}\,\dot{M}_{\rm BH}\,c^2. \tag{34}$$

Characteristically, we take $\epsilon_{\rm f} \sim 0.05$, so that ~0.5 per cent of the accreted rest mass energy is available as feedback. This value fixes the normalization of the $M_{\rm BH}$–$\sigma$ relation and brings it into agreement with current observations (Di Matteo, Springel & Hernquist 2005).

© 2005 RAS, MNRAS **361,** 776–794

# *Other Accretion Methods*

- Debuhr, Quataert, Ma & Hopkins 2010, MNRAS, 406, L55

We estimate the accretion rate onto the BH from the surrounding gas, due to viscous transport of angular momentum, using

$$\dot{M}_{vis} = 3\pi\alpha\Sigma\frac{c_s^2}{\Omega}\,, \qquad (2)$$

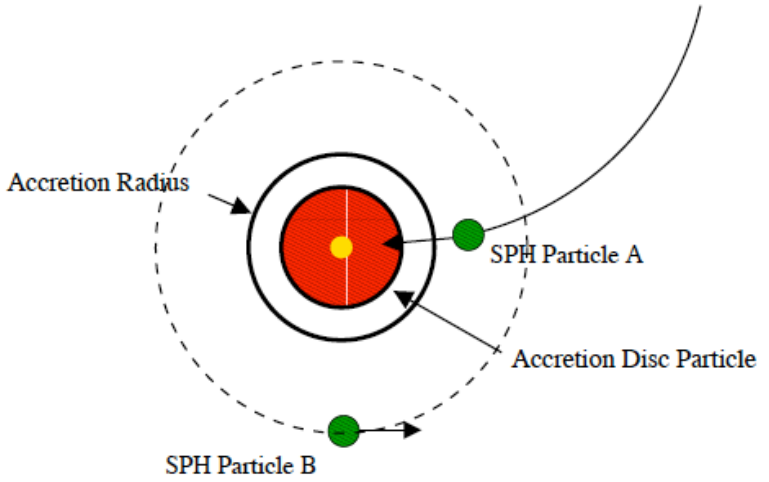


**Figure 1. The Accretion Disc Particle Method.** The accretion disc particle is a collisionless sink particle that consists of a black hole and its accretion disc. SPH particle A has a small angular momentum and so its orbit brings it within the accretion disc particle's accretion radius $R_{\rm acc}$, at which point it is added to the accretion disc. SPH particle B's angular momentum is too large for it to be captured. The black hole feeds from the accretion disc on a viscous timescale $t_{\rm visc}$. Both $R_{\rm acc}$ and $t_{\rm visc}$ are free parameters in the accretion disc particle method.

- Power, Nayakshin & King 2010, arXiv: 1003.0605

# *Feedback*

- *Small-scale SMBH accretion work indicate lower $\varepsilon_f \Rightarrow$*

  Kurosawa, Proga & Nagamine (2009, ApJ, 707, 823)

- Ostriker et al. (2010, ApJ, 722, 642)
  - Momentum Driving

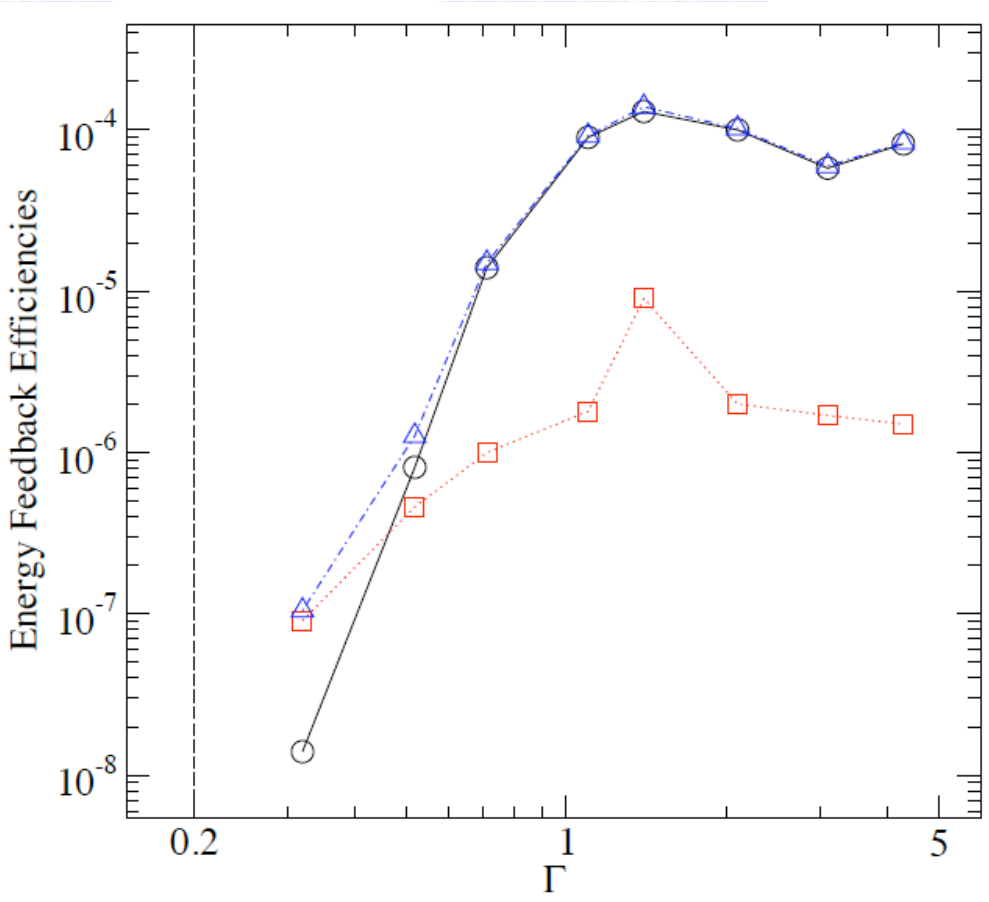


FIG. 4.— The efficiencies of converting the BH accretion luminosity $L_a$ to the rate of energy deposition to the surrounding gas are plotted as a function of the Eddington ratio ($\Gamma$). The panel shows the kinetic energy feedback efficiency $\epsilon_k$ (*circles*), the thermal energy feedback efficiency $\epsilon_{th}$ (*squares*) and the total energy feedback efficiency $\epsilon_t = \epsilon_k + \epsilon_{th}$ (*triangles*), separately (see Eqs. [4], [5], and [6]). The maximum total energy feedback efficiency is $\sim 10^{-4}$. For the models with relatively low Eddington ratio ($\Gamma \lesssim 0.4$), the thermal feedback is more efficient than the kinetic feedback ($\epsilon_{th} > \epsilon_k$). For the models with relatively high Eddington ratio ($\Gamma \gtrsim 0.6$), the kinetic feedback is more efficient than the thermal feedback by a factor of $\sim 10$ to $\sim 100$. The model with $\Gamma = 0.2$ does not form an outflow, and the vertical line (*dashed*) at $\Gamma = 0.2$ indicates an

# *AGN Feedback Invoked to Resolve Issues in Galaxy Formation Models*

- Galaxy properties regulated by SMBH
  - (Salpeter 1964, Lynden-Bell 1969, Rees 1984, Silk & Rees 1998, Best 2007)
- SMBH - host galaxy bulge correlations
  - (Di Matteo et al. 2005, 2008)
- Quench star-formation in galaxies
  - (Springel et al. 2005, Bower et al. 2006, Croton et al. 2006, Johansson et al. 2008, Antonuccio-Delogu & Silk 2008)

- Redshift evolution (sharp cutoff at the bright end) of galaxy luminosity function
- Anti-hierarchical turn-off in QLF at low-z
  - Thacker et al. 2006

- Galaxy cluster
  - Heat up the ICM & stop cooling-flow
    - (McNamara & Nulsen 2007)
  - Pre-heating (entropy floor in cool-core clusters)

# *AGN Outflows in a Cosmological Volume & IGM Enrichment*

Collaborators: Hugo Martel, Joël Germain
Université Laval
Québec City, Canada


# Introduction

- Outflows observed in a large fraction of AGN
  - (Crenshaw et al. 2003, Everett 2007, Nesvadba et al. 2008)

- Influence large-scale-structures
  - Enrich IGM with metals → modify cooling rate of star-forming gas
  - Heat / displace / compress proto-galactic gas → affect further star / galaxy formation

- Goal :

  Investigate impact of AGN outflows on
  - Metal enrichment of the IGM
  - Volume fraction of the Universe enriched, Metallicity

# Observed IGM Metallicity

- Average $Z_{IGM} \geq 10^{-3}\ Z_{\odot}$ by $z \sim 2 - 3$
- CIV lines
  - (Cowie et al. 1995, Songaila 1997, 2001, D'Odorico et al. 2010)
- OVI lines: $10^{-3} - 10^{-1.5}\ Z_{\odot}$ at $z \sim 2 - 2.5$
  - (Bergeron et al. 2002, Simcoe et al. 2004)
- $Z_{IGM} \geq 10^{-2.4}\ Z_{\odot}$ at $z = 0.9$ (Burles & Tytler 1996)
- In local-universe:

  $[C/H] \approx -1.2$, & $[O/H] \geq -2$ (Tripp et al. 2002)
- $\leq 2.5 - 10\ \%\ Z_{\odot}$ (Shull et al. 2003), $Z_O \sim 0.09\ Z_{\odot}$ (Danforth & Shull 2005)

➢ Mechanism: Winds (starburst / SNe / AGN - driven) can heat, ionize & enrich IGM
  - Voit (1996)

# AGN-driven

- Khalatyan et al. 2008: without AGN under-estimate $Z_{IGM}$ at overdensity<10, with AGN feedback (thermal) over-enrich
- Tornatore et al. 2010: BH feedback provides stronger and more-pristine enrichment of warm-hot IGM
- Metal spreading by expanding lobes of Radio Galaxies
  - Analytical: Gopal-Krishna & Wiita 2001, Barai & Wiita 2007
  - Observation: Kirkpatrick et al. 2009
- Enriching the ICM in galaxy clusters: Moll et al. 2007, Sijacki et al. 2008, Fabjan et al. 2010

# Motivation

- Previous studies on cosmological impact of AGN outflows
  - Furlanetto & Loeb 2001, ApJ, 556, 619
  - Scannapieco & Oh 2004, ApJ, 608, 62
  - Levine & Gnedin 2005, ApJ, 632, 727
  - Barai, 2008, ApJ, 682, L17

Spherical Outflow

Our Improvement

- Anisotropically expanding outflow
- Track enrichment history of IGM

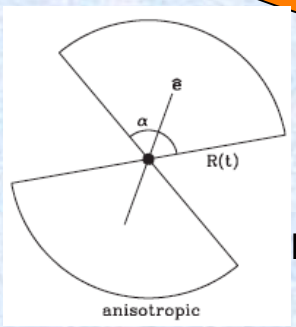

# Methodology

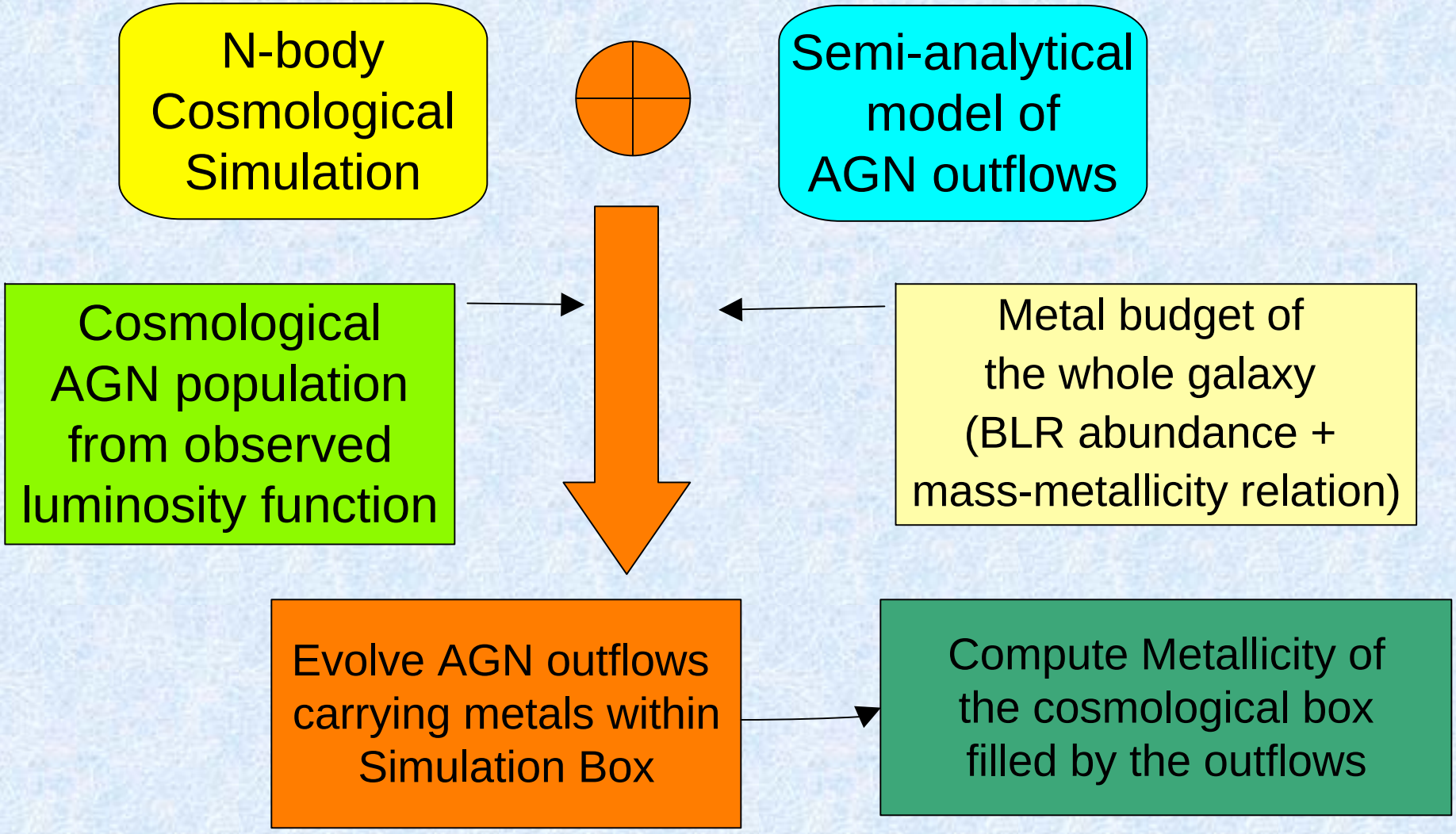

# Cosmological Simulation

- N-body simulations of a cosmological volume
- $P^3M$ (particle-particle/particle-mesh) code

- Box size (comoving) = 128 $h^{-1}$ Mpc
- $256^3$ particles, $512^3$ grid
- Evolve from $z = 25$ up to $z = 0$
- $\Lambda$CDM model (WMAP5)

- Assume: baryonic gas distribution follows total matter in the simulation box

# Redshift & Luminosity Distribution

- Observed AGN bolometric luminosity function
  (Hopkins, Richards & Hernquist 2007, ApJ, 654, 731)

$$\varphi(L) = \frac{\varphi_*}{(L/L_*)^{\gamma_1} + (L/L_*)^{\gamma_2}}$$

- Fraction of AGN hosting outflows = 0.6
  - (Ganguly, R. & Brotherton, M.S. 2008, ApJ, 672, 102)

- Using, AGN lifetime, $T_{AGN} = 10^8$ yr,
  Total number of sources from QLF = 1,535,362

- Locate AGN at local density peaks within simulation volume

# All Sources in Box from QLF. $N_{AGN,total}$ = 1535362.

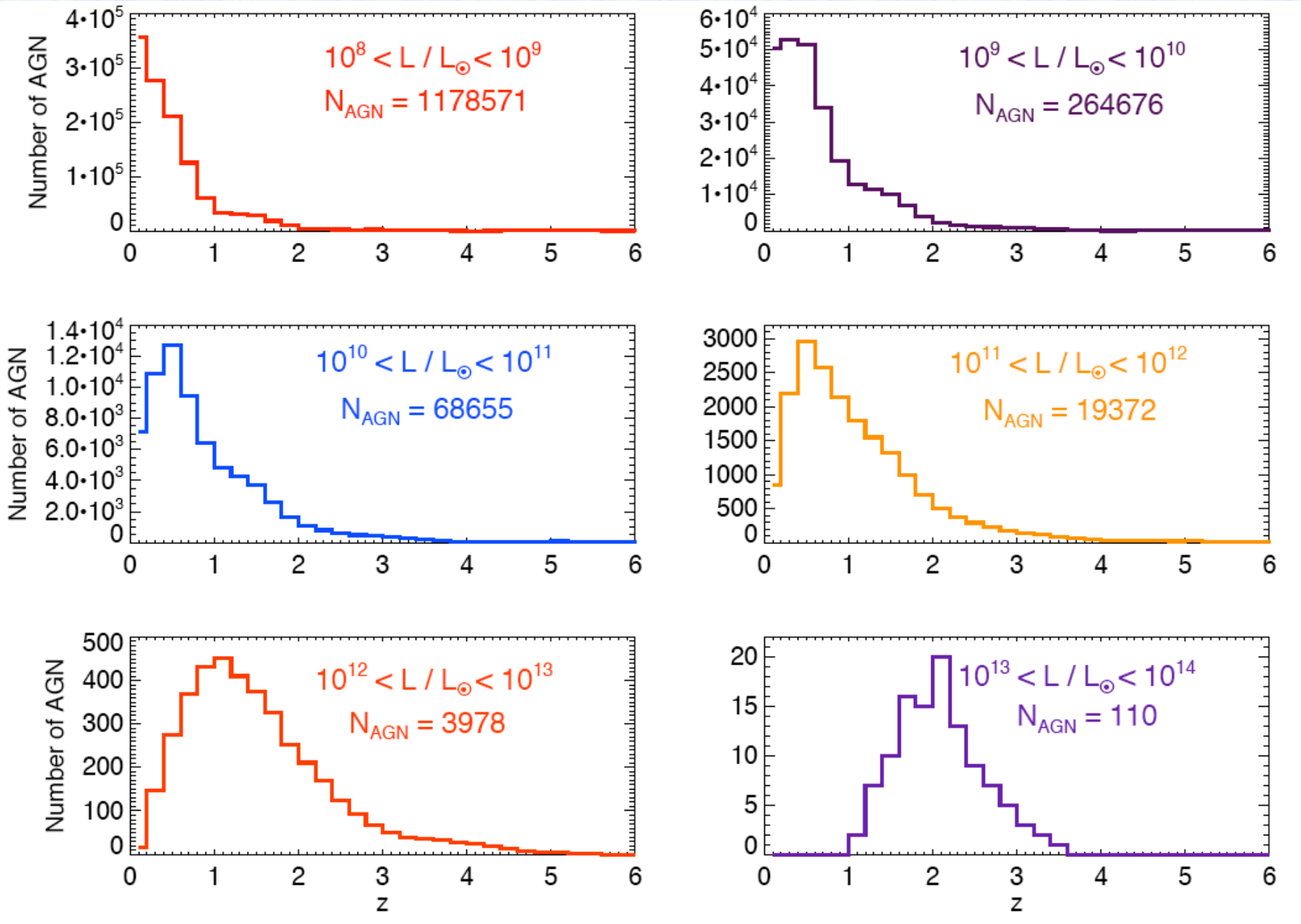

# Outflow Geometry

- Bipolar Spherical Cone (Pieri, Martel & Grenon 2007, ApJ, 658, 36)

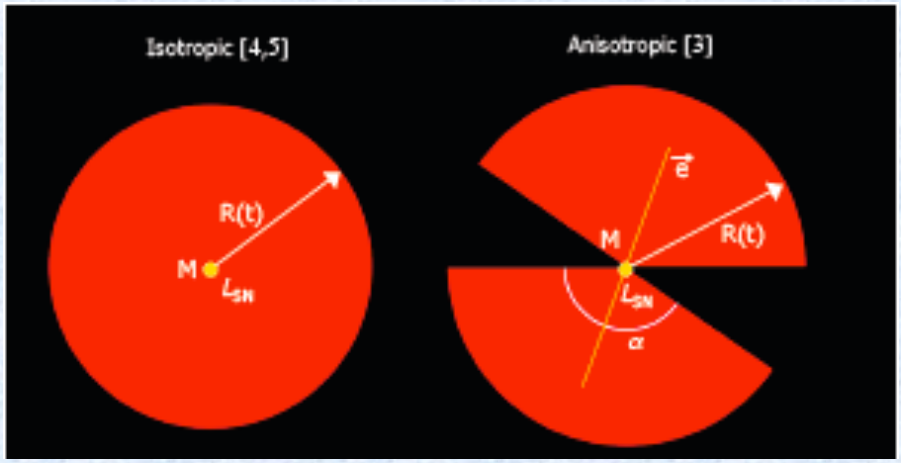


$$r \le R$$
$$0 \le \theta \le \frac{\alpha}{2} \text{ ,or, } \left(\pi - \frac{\alpha}{2}\right) \le \theta < \pi$$
$$0 \le \phi < 2\pi$$

$$V = \frac{4}{3}\pi R^3 \left(1 - \cos\frac{\alpha}{2}\right)$$

- Expands anisotropically in large scales
  - Away from over-dense regions, into under-dense regions
  - Follows path of Least Resistance --- Direction along which density drops the fastest
  - (Martel & Shapiro 2001, RevMexAA, 10, 101)

# Ambient Medium for AGN Outflows

- Assume: baryonic gas distribution follows dark matter in the simulation box
- Gas density : $$\rho_x(z,\vec{r}) = \frac{\Omega_B}{\Omega_M}\rho_M(z,\vec{r})$$
- Pressure : $$p_x(z,\vec{r}) = \frac{\rho_x(z,\vec{r})KT_x}{\mu}$$
- Temperature (assuming a photoheated medium) $$T_x = 10^4 \text{ K}$$
- Mean molecular mass : $$\mu = 0.611 \text{ a.m.u.}$$

# Semi-analytical Model

- Outflow expansion :

$$\ddot{R} = \frac{4\pi R^2}{M_S}\left(1-\cos\frac{\alpha}{2}\right)\left(p_T + p_B - p_x\right) - \frac{G}{R^2}\left(M_d + M_{gal} + \frac{M_S}{2}\right) + \Omega_\Lambda H^2 R - \frac{\dot{M}_S}{M_S}\left(\dot{R} - v_p\right)$$

Pressure gradient — Gravitational deceleration — Cosmological constant — Drag force

- Thermal pressure :

$$\dot{p}_T = \frac{\Lambda}{2\pi R^3\left[1-\cos(\alpha/2)\right]} - 5\,p_T\,\frac{\dot{R}}{R}$$

Thermal energy injection — Outflow expansion

- Magnetic pressure :

$$\dot{p}_B = \frac{\varepsilon_B L_{AGN}}{4\pi R^3\left[1-\cos(\alpha/2)\right]} - 4\,p_B\,\frac{\dot{R}}{R}$$

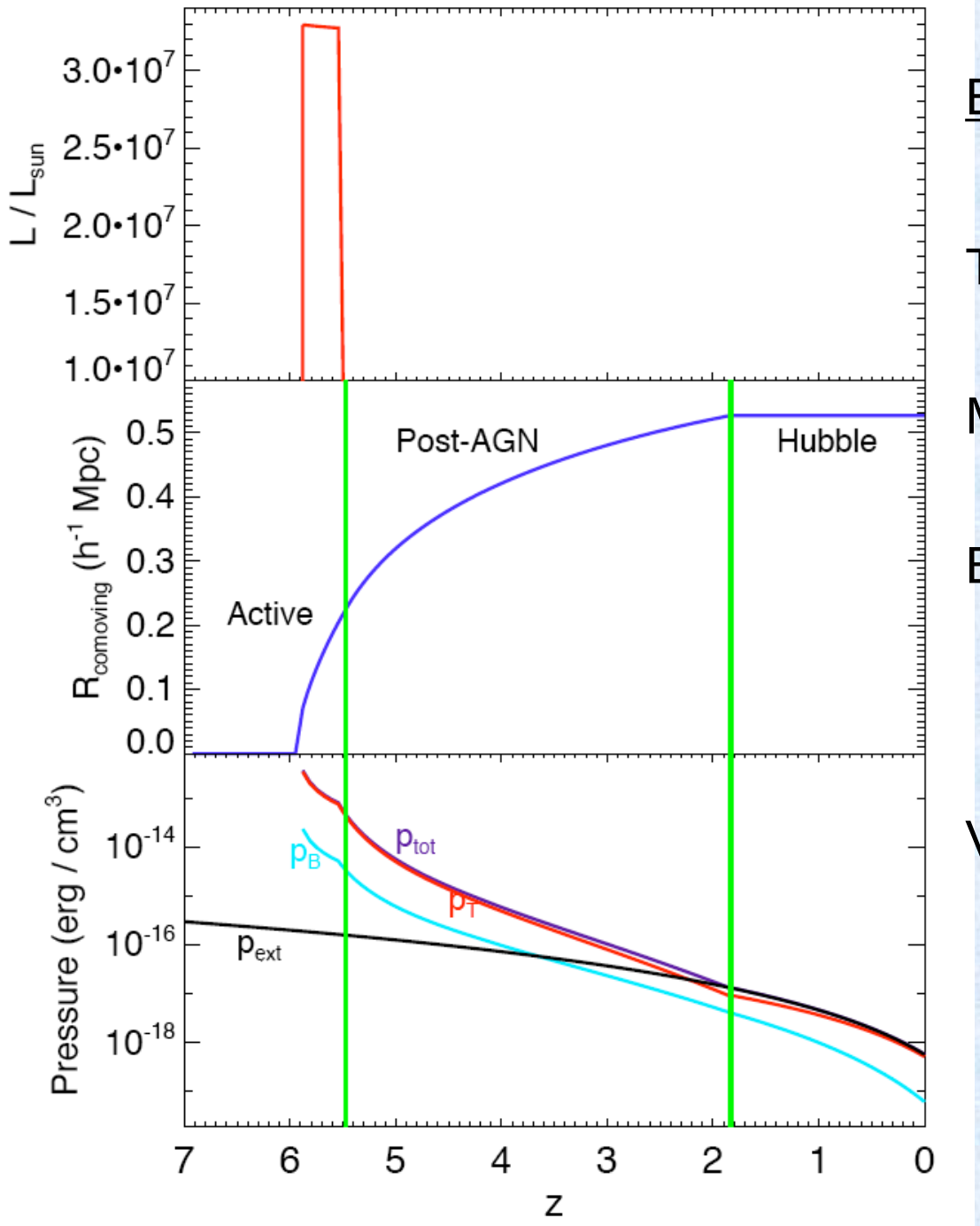


## Evolution of a single outflow

Top: total luminosity.

Middle: Comoving radius.

Bottom: Pressures (external IGM, magnetic, thermal and total outflow).

Vertical green lines separate phases of expansion: active, post-AGN and Hubble.

# Metal Enrichment

- AGN outflows carry the metals produced by their host galaxies, & deposit those to the surrounding IGM volume

- Particles (of $P^3M$ code) intercepted by each outflow volume are flagged as enriched
  - For all the outflows existing in the box
  - At every redshift

  $\Rightarrow$ Enrichment history of IGM

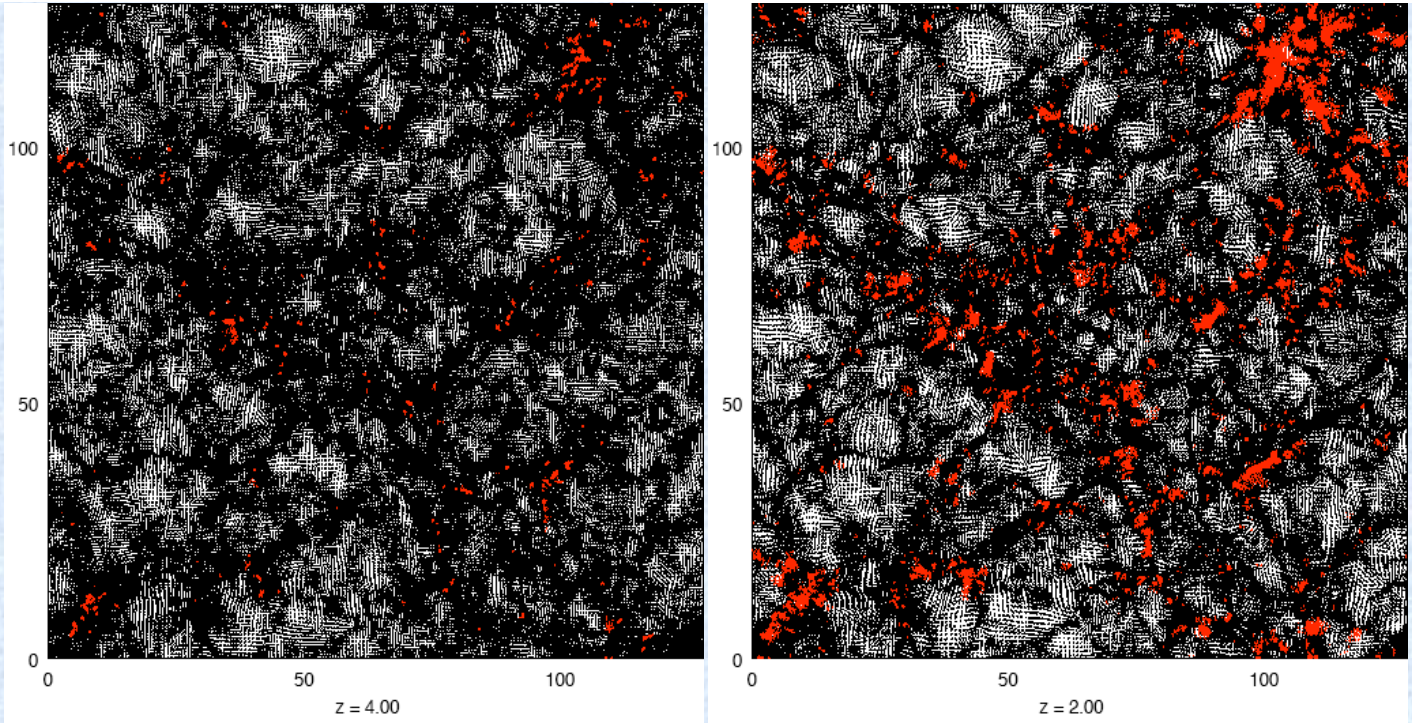


A slice of the box (128/h Mpc × 128/h Mpc × 4/h Mpc) at different redshifts.

Black dots: Non-enriched particles.

Red dots: Enriched particles.

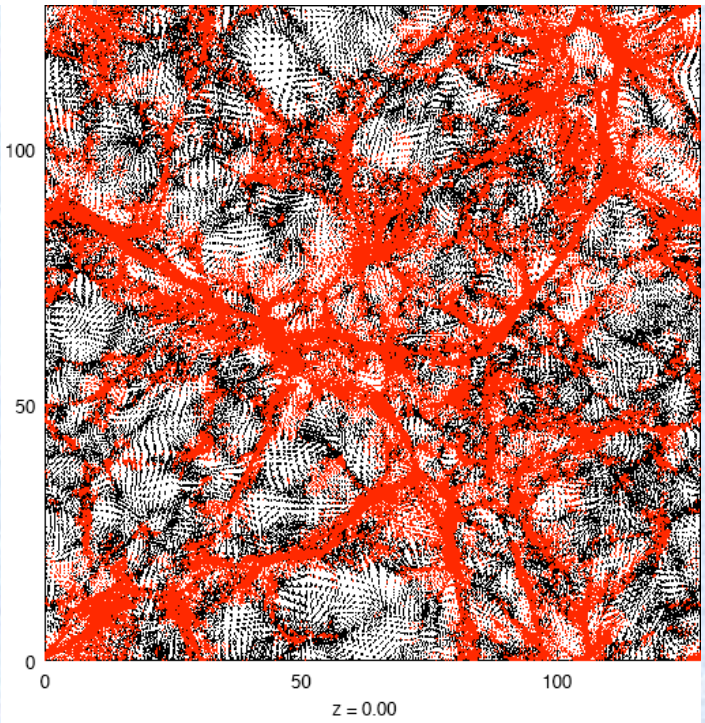

# Compute IGM Volume Enriched

- Use SPH smoothing algorithm
  $\Rightarrow$ Get density on a grid $N_{ff}^3 = 256^3$
- Each particle
  - Ascribed a Smoothing Length $h$
  - Extends over a spherical volume of radius $1.7h$

- Count mesh cells (of $N_{ff}$ grid) occurring inside the spherical volume of one/more enriched particles
- Total number of enriched cells, $N_{AGN}$
  $\Rightarrow$ Enriched volume of box
- Volume fraction of box enriched by outflows
  $= N_{AGN} / N_{ff}^3$

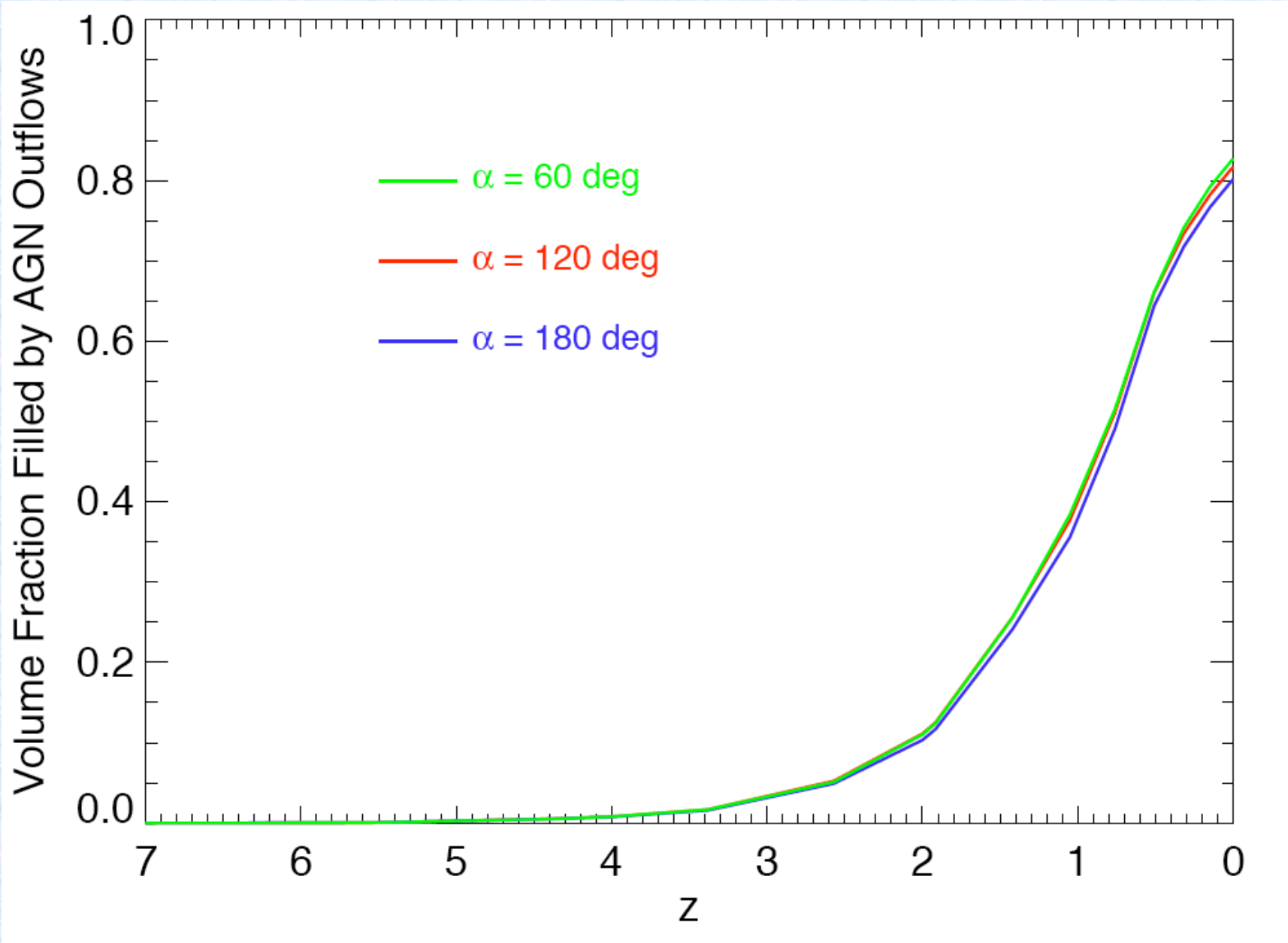


Volume fractions enriched (for different opening angles)

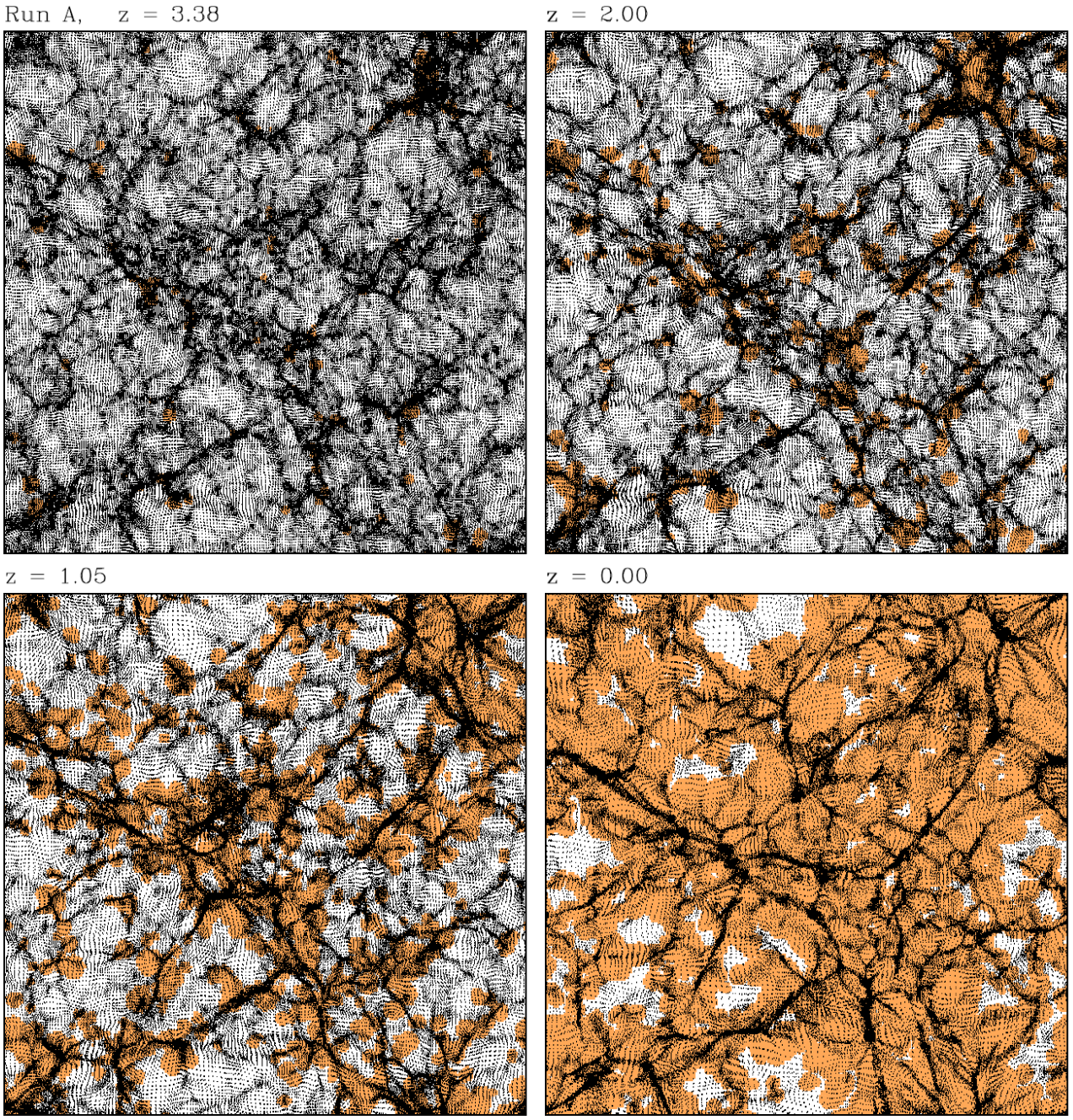


Evolution of metal distribution in a slice (128/h Mpc × 128/h Mpc × 2/h Mpc).

Orange : enriched volumes.

Black dots : $P^3M$ particles, showing the large-scale structures.

**$\alpha$ = 180°**

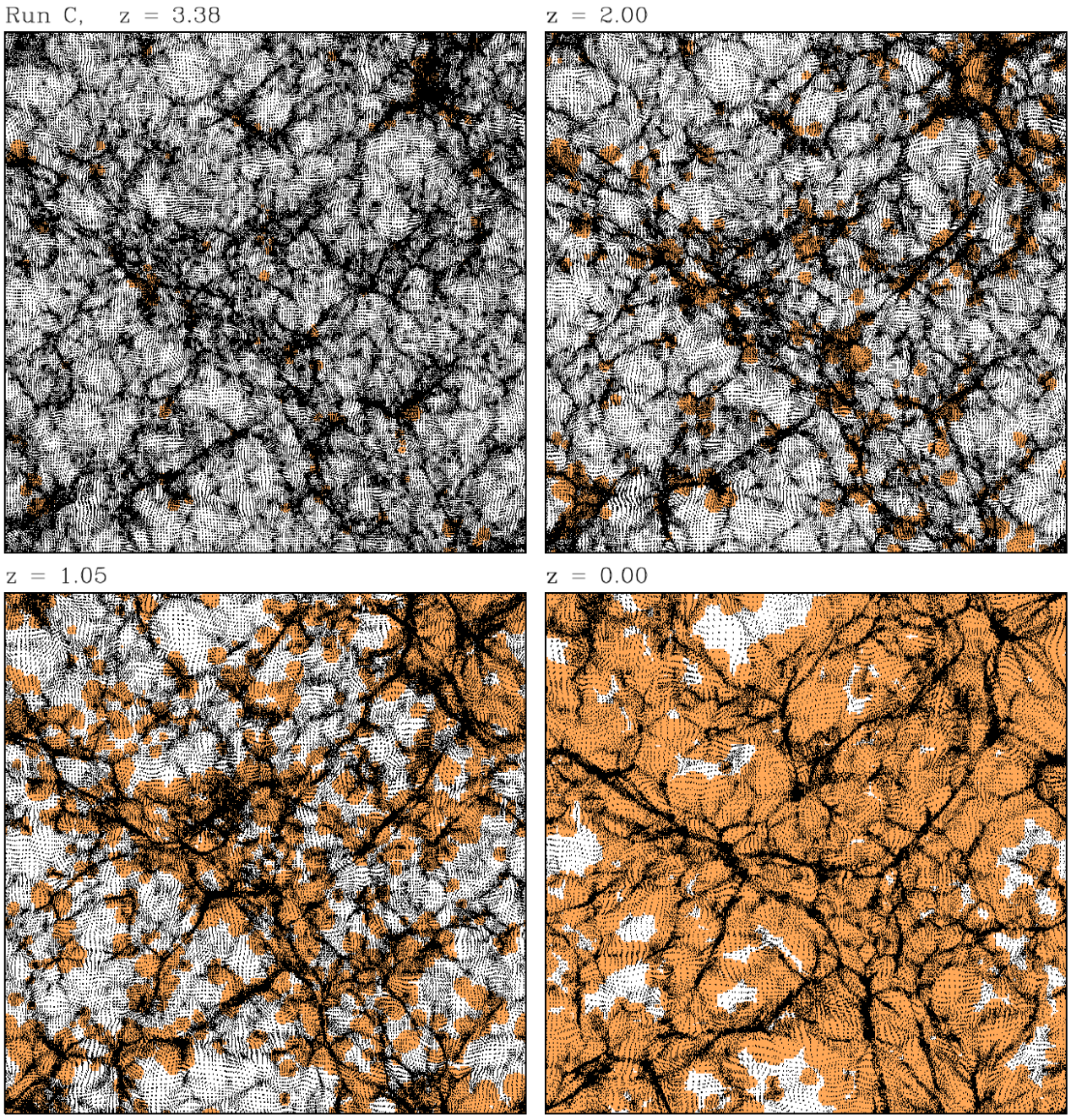


Evolution of metal distribution in a slice (128/h Mpc × 128/h Mpc × 2/h Mpc).

Orange : enriched volumes.

Black dots : $P^3M$ particles, showing the large-scale structures.

**$\alpha$ = 60°**

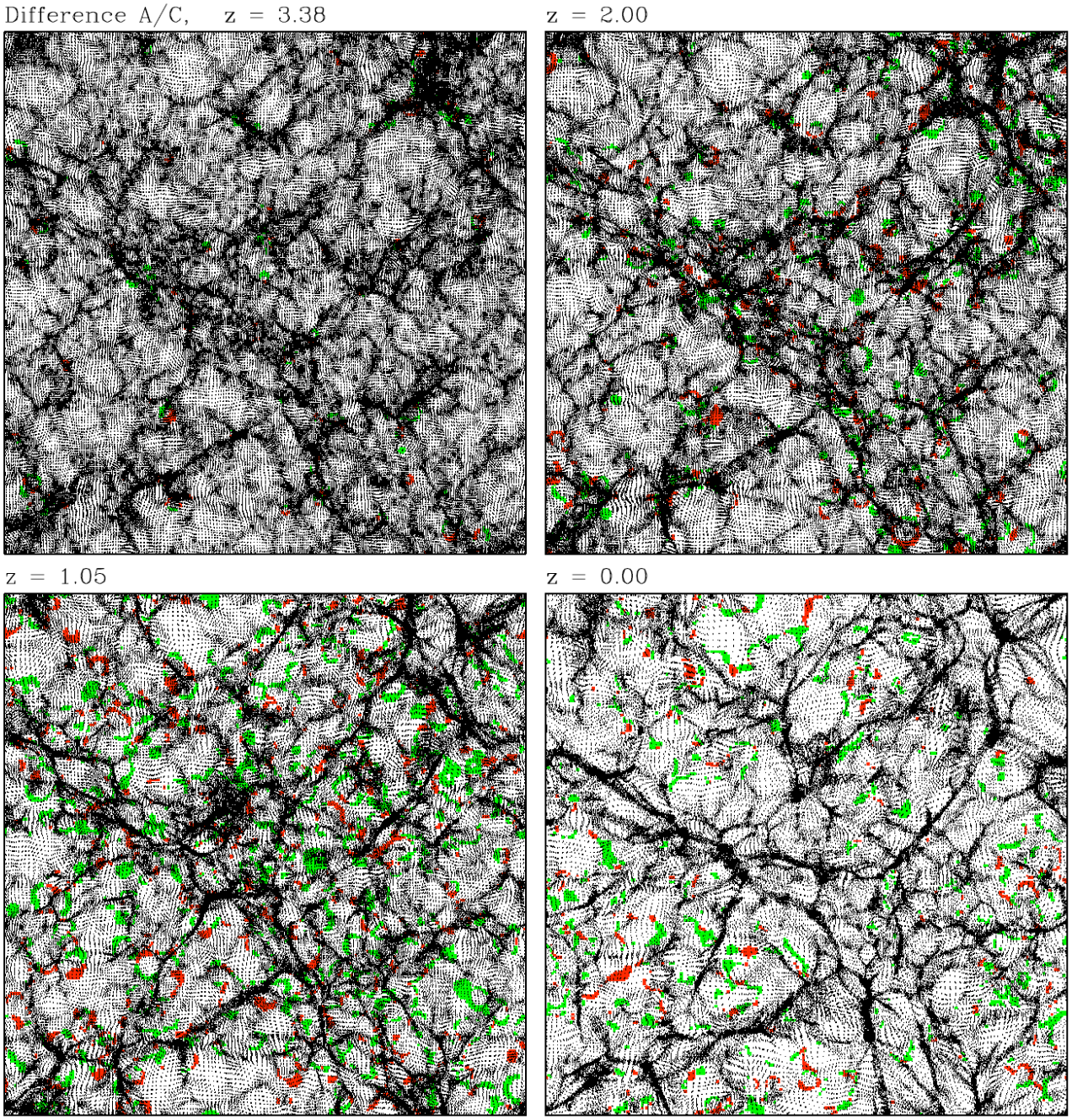


Differential enrichment map between $\alpha = 180°$ and $\alpha = 60°$.

Red : regions enriched with 180°, but not 60°.

Green : regions enriched with 60°, but not 180°.

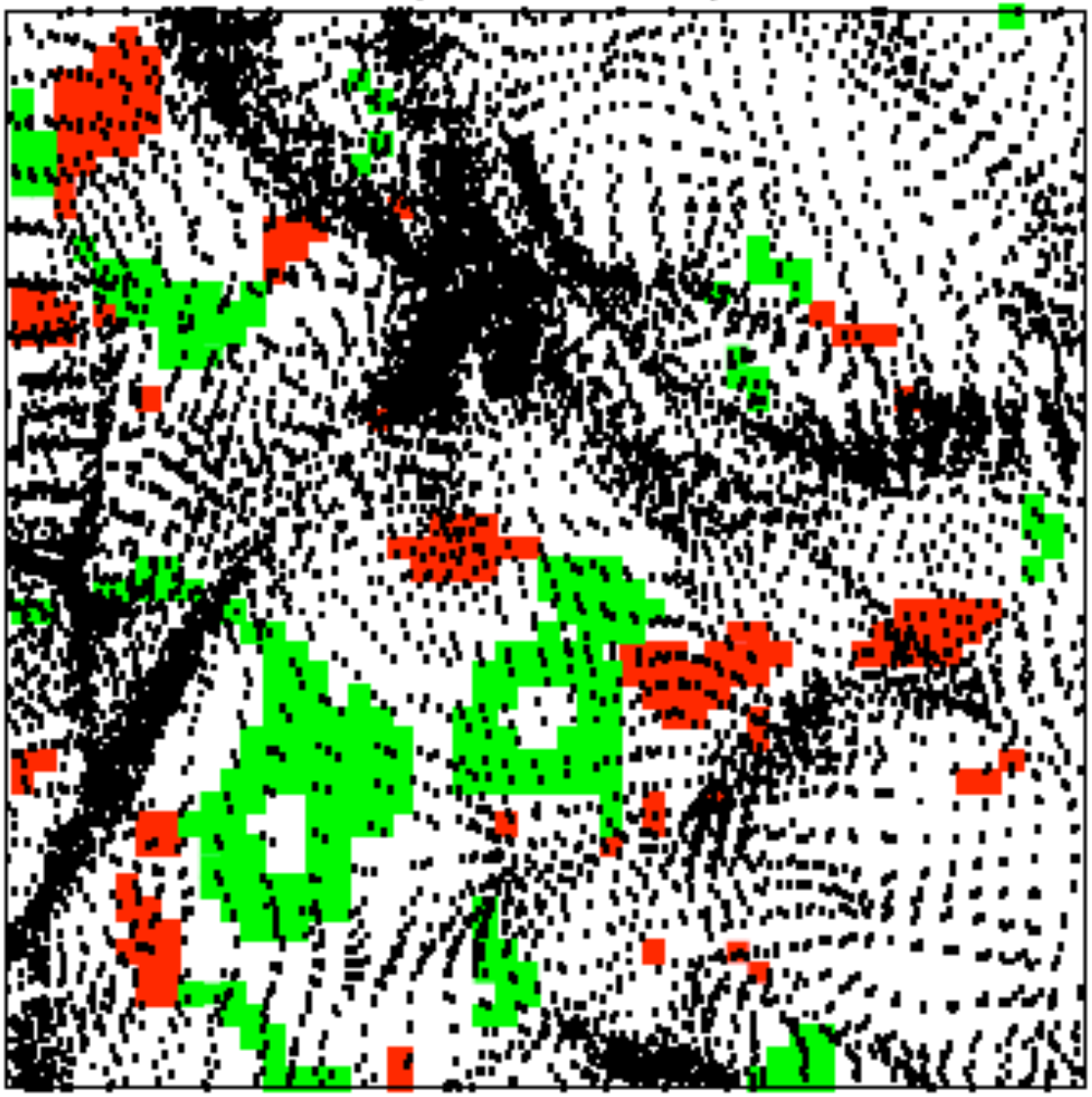


Differential enrichment map between $\alpha = 180°$ and $\alpha = 60°$.

Red : regions enriched with 180°, but not 60°.

Green : regions enriched with 60°, but not 180°.

$z$ **= 1.05**

Green areas tend to be in more underdense regions than red areas.

# Parameters of Simulation Runs & Final Enriched Volume Fractions

| Run | $\alpha$ (°) | $T_{\rm AGN}$ (yr) | $\epsilon_K$ | Bias in Location | $N_{\rm rich}/N_{\rm ff}^3(z=0)$ |
|---|---|---|---|---|---|
| A | 180 | $10^8$ | 0.10 | × | 0.80 |
| B | 120 | $10^8$ | 0.10 | × | 0.82 |
| C | 60 | $10^8$ | 0.10 | × | 0.83 |
| D | 60 | $10^7$ | 0.10 | × | 1.00 |
| E | 60 | $10^9$ | 0.10 | × | 0.75 |
| F | 60 | $10^8$ | 0.05 | × | 0.79 |
| G | 60 | $10^8$ | 0.01 | × | 0.71 |
| H | 60 | $10^8$ | 0.10 | √ | 0.75 |
| I | 60 | $10^8$ | 0.10 | √ | 0.65 |

# Compute Metallicity: Mass of Metals in Galaxy

- Metals generated in galaxies are transported to the IGM
- 2 regions of stellar populations:

1) Near the AGN (central regions)

$$M_{Z,1} = \left(5 Z_{\mathrm{Sun}}\right) M_{BH}$$

(Hamann & Ferland 1992, Dietrich et al. 2003)

2) Away from central AGN (within rest of the galaxy)

$$M_{Z,2} = f_{esc} Z_G \left(1 - f_*\right) M_{gal}$$

- Redshift-dependent mass-metallicity relation (Maiolino et al. 2008, A&A, 488, 463)

$$12 + \log\left(\frac{O}{H}\right) = -0.0864\left(\log M_* - \log M_0\right)^2 + K_0$$

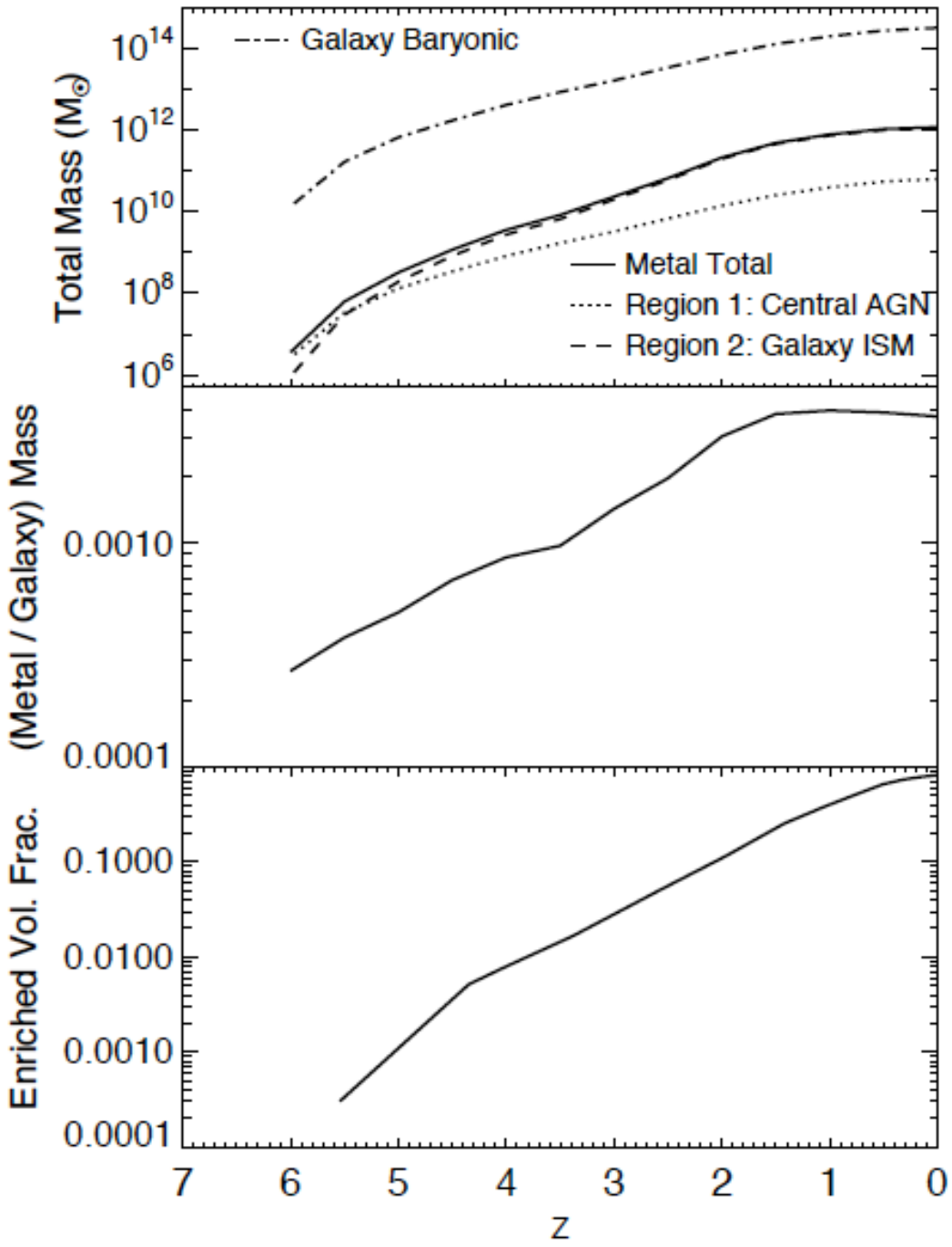


Quantities in whole Simulation Volume

# Distribution of Metals from Galaxy to IGM

- Total mass of metals carried is deposited uniformly into the IGM gas overlapped by the outflow

$$M_{Z,out} = M_{Z,1} + M_{Z,2}$$

- All the metals are added to the IGM by the active lifetime
- Metals are redistributed (conserving total metal mass, using an averaging technique) to the larger volumes overlapped in the post-AGN overpressured expansion, until the outflow reaches the passive Hubble flow evolution

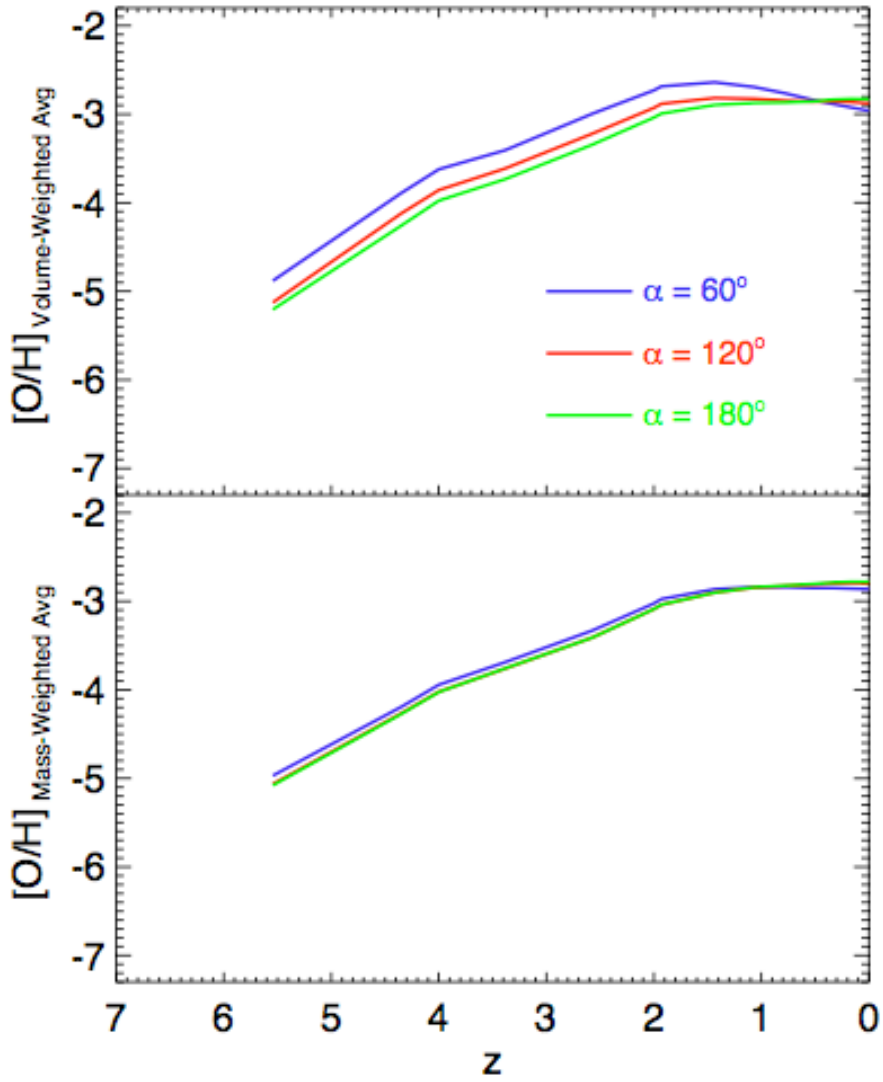


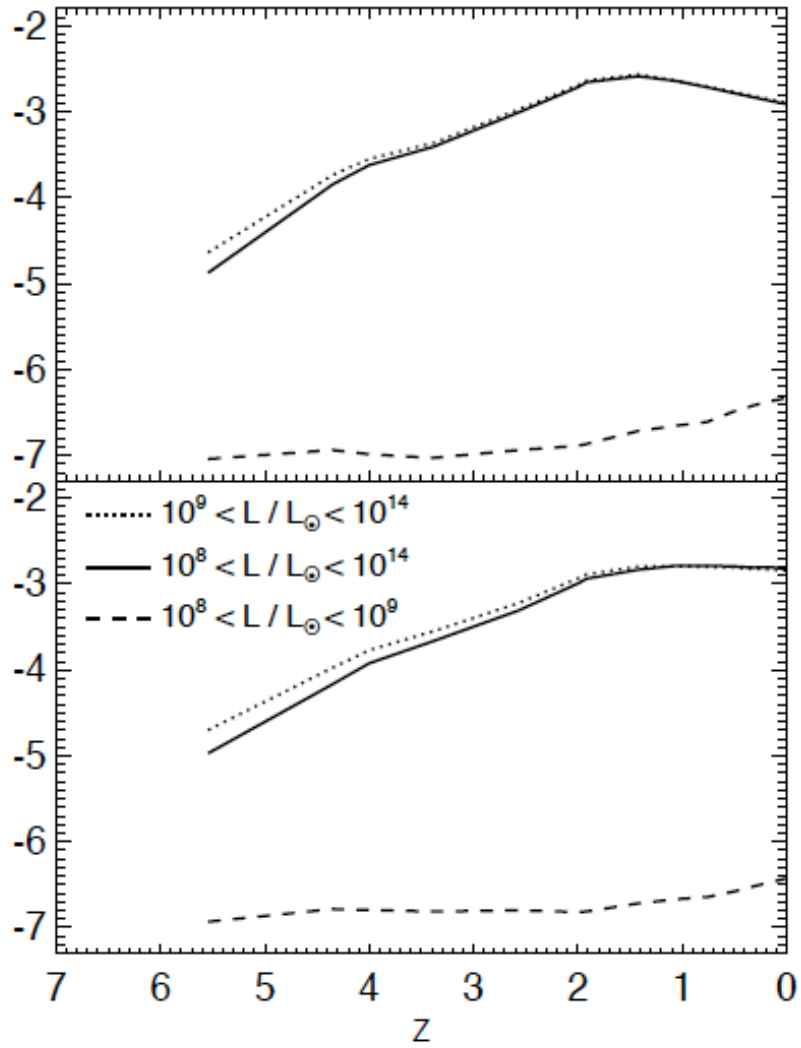


Average IGM metallicity of [O/H] = −5 is produced at z = 5.5, which then rises gradually, and remains relatively flat at [O/H] = −2.8 between z = 2 and z = 0.

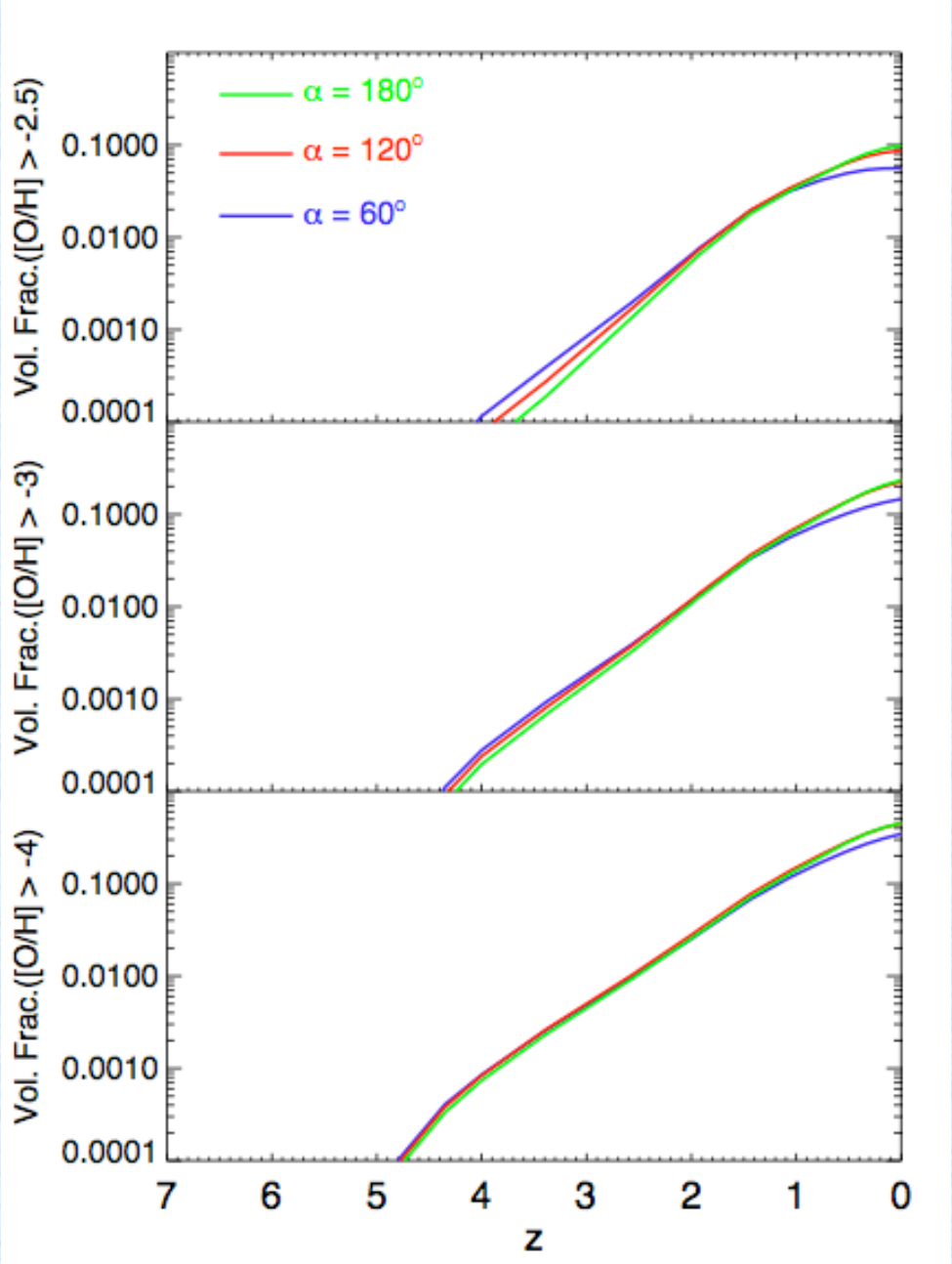


Enriched volume fractions are small at $z > 3$, then rises rapidly to the following at $z = 0$:

6−10% of the volume enriched to $[O/H] > -2.5$,

14−24% volume to $[O/H] > -3$,

34−45% volume to $[O/H] > -4$.

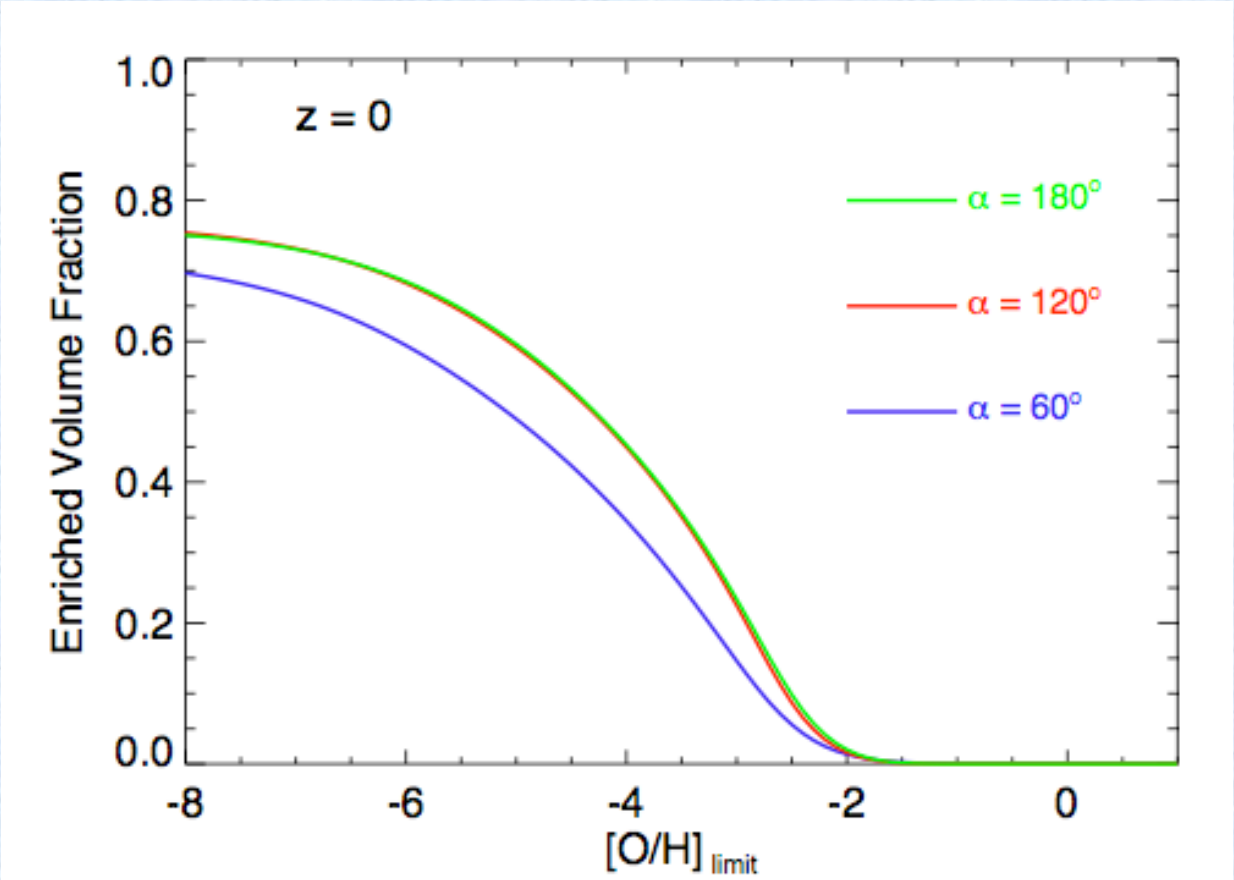


Volume fractions enriched above a certain metallicity limit, $V([O/H] > [O/H]_{limit})$, at the present epoch.

More than 60% of the volume is enriched to [O/H] > −6, and 1−2% of the volume is enriched to [O/H] > −2.

# Contribution to the IGM Metallicity

- CIV and OVI observations
  - (Songaila 2001, ApJ, 561, L153)
  - (Simcoe, Sargent & Rauch 2004, ApJ, 606, 92)

$$Z_{IGM} \sim 10^{-4} Z_{\mathrm{Sun}}, \text{ at } z = 5$$
$$\geq 10^{-3} - 10^{-2} Z_{\mathrm{Sun}}, \text{ at } z \sim 2 - 3$$
$$\geq 10^{-2} - 10^{-1} Z_{\mathrm{Sun}}, \text{ at low} - z$$

- Propagation of metals by AGN outflows contribute a fraction (10 - 20 %) of the observed IGM metals
  - Do not account for 100%

- Observations of radio galaxy MRC 1138-262
  - (Nesvadba et al. 2006, ApJ, 650, 693)
  - AGN feedback from massive galaxies may account for few to 20% of all IGM metals at z ~ 2

- Simulations must count metals ejected by outflows driven by SNe or starbursts, from dwarf & low-mass galaxies, at high-z ($6 < z < 15$)
  - (Scannapieco, Ferrara & Madau 2002, ApJ, 574, 590)
  - (Oppenheimer & Dave 2006, MNRAS, 373, 1265)

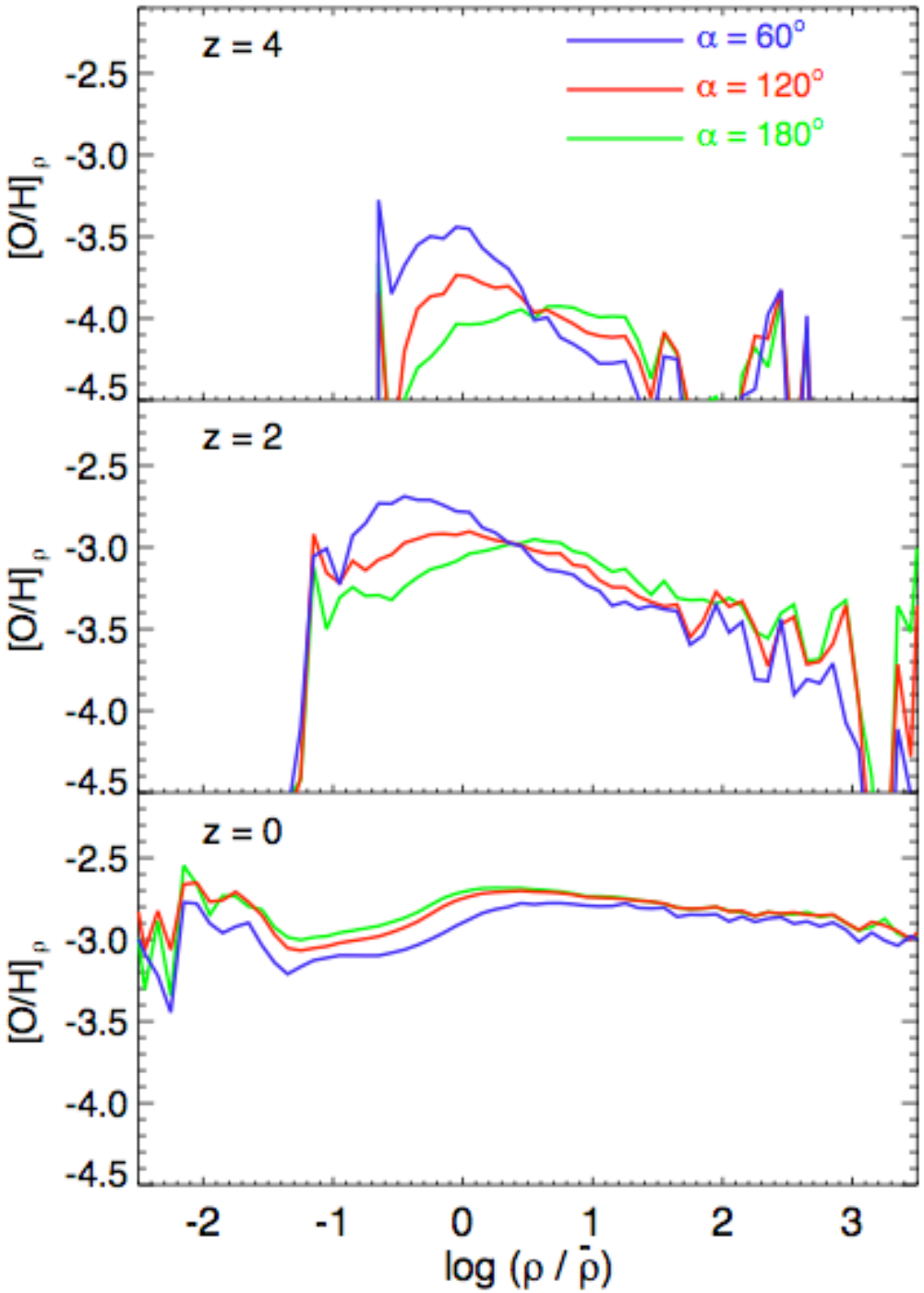


Metallicity (at a given density) as a function of the total density of the IGM.

Initially, more anisotropic outflows preferentially enrich low-density regions,

but this trend gets eventually washed-out as the enriched volume fraction approaches unity.

# Summary & Conclusions

- Implemented a semi-analytical model of anisotropic AGN outflows in N-body simulations

- The resulting filled volume fractions are relatively small at $z > 2.5$,

  then grow rapidly afterward to 65 – 100% volume (for different model parameters) of the Universe permeated by the present

- IGM is metal-enriched to ~ 10 - 20 % of the observed metallicity, the result depending on redshift

- Increasingly anisotropic outflows preferentially enrich under-dense regions, esp. at higher redshifts
  - Can explain observations of enriched low-density IGM at $z \sim 3 - 4$

# References


- Barai, P., Martel, H. & Germain, J. 2011, ApJ, 727, 54
- Germain, J., Barai, P. & Martel, H. 2009, ApJ, 704, 1002
- Martel, H. & Shapiro, P.R. 2001, RevMexAA, 10, 101
- Pieri, M. M., Martel, H. & Grenon, C. 2007, ApJ, 658, 36

# Extra Slides

# Galactic Outflows (SNe-driven)

- Tegmark et al. (1993): IGM enriched to 10% of current by z=5
- Aguirre et al. (2001): cosmological simulation, 200-300 km/s wind at z ≥ 3 can enrich to obs values, but low-density IGM metal-free
- Some studies show only a fraction of IGM metals by SN-winds: Gnedin (1998), Ferrara et al. (2000)
- Enrichment is inhomogeneous - strongly dependent on density (Cen & Ostriker 1999, Schaye et al. 2003)
- Scannapieco et al. (2002): 30% volume enriched to 10–3 Z¤ at z=3
- Thacker et al. (2002): 20% to 0.003 Z¤ at z=4
- Oppenheimer et al. (2009): 1% to >10–3 Z¤ at z=5
- Shen et al. (2010) …

# Direction of Least Resistance (DLR)

- In large-scale filamentary structures, outflow direction is obtained from pressure of surrounding medium

<u>Implementation</u>

- Find DLR around density peaks
- Taylor expansion of density around a peak inside sphere of radius R★
- Rotate Cartesian coordinates to make cross-terms vanish

$$\delta(x',y',z') = \delta_{peak} - Ax'^2 - By'^2 - Cz'^2$$

- Largest of the coefficients A, B, C $\Rightarrow$ DLR